December 22, 2014

An Experimental Program in Neutrinos, Nucleon Decay and Astroparticle Physics Enabled by the Fermilab Long-Baseline Neutrino Facility

Letter of Intent Submitted to the Fermilab PAC

December 22, 2014

Table of Contents

An Experimental Program in Neutrinos, Nucleon Decay and Astroparticle Physics Enabled by the Fermilab Long-Baseline Neutrino Facility

1.0 Executive Summary and Introduction

1.1 Executive Summary

This is a Letter of Intent (LOI) by a global neutrino community to pursue an accelerator-based long-baseline neutrino experiment, as well as neutrino astrophysics and nucleon decay, with an approximately 40-kt (fiducial mass) modular liquid argon TPC (LAr-TPC) detector located deep underground and a high-resolution near detector. Several independent worldwide efforts, developed through many years of detailed studies, have now converged around the opportunity provided by the megawatt neutrino beam facility planned at Fermilab and by the new significant expansion with improved access foreseen at the Sanford Underground Research Facility in South Dakota, 1,300 km from Fermilab.

The principle goals of this experiment are: to carry out a comprehensive investigation of neutrino oscillations to test CP violation in the lepton sector, determine the ordering of the neutrino masses, and to test the three-neutrino paradigm; to perform a broad set of neutrino scattering measurements with the near detector; and to exploit the large, high-resolution, underground far detector for non-accelerator physics topics including atmospheric neutrino measurements, searches for nucleon decay, and measurement of astrophysical neutrinos especially those from a core-collapse supernova.

The new international team has the necessary expertise, technical knowledge, and critical mass to design and implement this exciting discovery experiment in a relatively short timeframe. The goal is the deployment of the first 10-kt fiducial mass detector on the timescale of 2021, followed by future expansion to the full detector size as soon as possible. The PIP-II accelerator upgrade at Fermilab will provide 1.2 MW of power by 2024 to drive a new neutrino beam line at Fermilab. There also exists a plan that could further upgrade the Fermilab accelerator complex to enable it to provide up to 2.4 MW of beam power by 2030. With the availability of space for expansion and improved access at the Sanford laboratory, this international collaboration will develop the necessary framework to design, build and operate a world-class deep-underground neutrino and nucleon decay

observatory. Fermilab will act as the host laboratory. This plan is aligned with the European Strategy Report and the US HEPAP Particle Physics Project Prioritization Panel (P5) report.

1.2 Introduction

The study of the properties of the neutrino has provided many surprises, including the first evidence in particle physics of physics beyond the Standard Model of elementary particles and interactions. The phenomenon of neutrino oscillations, whereby they change flavor as they propagate through space and time, is now well established, as is the modification of these oscillations in their passage through matter. Important conclusions that follow from these discoveries include that neutrinos have mass and that the mass eigenstates are mixtures of the flavor eigenstates.

With the exception of the possible hints for the existence of sterile neutrinos, the current data can be described in terms of the three-neutrino paradigm, in which the quantum-mechanical mixing of three mass eigenstates produces the three known neutrino-flavor states. The mixing is described by the Pontecorvo-Maki-Nakagawa-Sakata (PMNS) matrix, a parameterization that includes a CP-violating phase.

Speculations on the origin of neutrino masses are wide-ranging. An attractive possibility is that neutrino masses are related to a new ultra-high-energy scale that may be associated with the unification of matter and forces. Such theories are able to describe the absence of antimatter in the Universe in terms of the properties of ultra-heavy particles as well as offering a description of cosmological inflation in terms of the phase transitions associated with the breaking of symmetries at the ultra-high-energy scale. Piecing together the neutrino-mass puzzle will require more precise and detailed experimental information. Long-baseline neutrino oscillation experiments are essential if the requisite neutrino transitions are to be measured with the necessary precision.

One of the primary questions that the experimental program outlined in this LOI seeks to answer is whether the oscillations of neutrinos differ from those of anti-neutrinos, testing whether CP symmetry is violated in the leptonic sector. It is known that the degree of CP violation that occurs in the interactions of quarks is insufficient to explain why our universe is composed entirely of matter rather than antimatter. In long-baseline neutrino oscillation experiments the rate of oscillations, the way the oscillation rate varies with energy, and the differences between neutrinos and antineutrinos can be exploited to observe CP violation in

the leptonic sector for the first time. In the three-neutrino paradigm, CP violation is determined by the value of a complex phase δ_{CP} in the PMNS matrix, whose sign is opposite for neutrinos and antineutrinos; CP violation occurs if the value of δ_{CP} is not zero (or π). Discovery of CP violation in the neutrino sector could have potentially profound implications for our understanding of the matter-antimatter asymmetry in the Universe.

Current neutrino oscillation data tell us about differences in the squared masses of the neutrino mass states, and about the sign of the mass-squared difference between two of the states, but not about the difference of those with respect to the third, which may be heavier (normal ordering) or lighter (inverted ordering) than the other two. Resolving this neutrino mass hierarchy ambiguity, along with precise measurements of neutrino mixing angles, would be a potent discriminator between various classes of models that attempt to describe physics beyond the standard model and would have significant theoretical and cosmological implications. It is also an important input into the interpretation of results from other future neutrino experiments. Long-baseline neutrino oscillation experiments can determine the mass ordering by exploiting the matter effect on the oscillation probabilities, which affects the electron-neutrino component of the neutrino beam, with different effect on neutrinos and antineutrinos, and with opposite sign depending on the mass ordering.

Even without CP violation, electron neutrinos and antineutrinos propagating through the Earth behave differently due to the fact that the material through which the beam passes contains electrons but no positrons. This effect must be distinguished from the differences that arise from true CP violation. To unfold these two effects from each other in a single experiment requires a baseline, the distance from the neutrino source to detector, of greater than 1000 km. Discrimination can be further enhanced, remaining ambiguities resolved, and the precision of the measurements improved, by measuring the oscillation spectrum as a function of neutrino energy, ideally covering both first and second oscillation maxima.

An important goal of the proposed experimental program is to measure other parameters of the PMNS matrix precisely and to test the three-neutrino paradigm and the validity of the PMNS matrix as the description of neutrino mixing and oscillations. This involves measurements of ν_μ disappearance and both ν_e and ν_τ appearance, with the goal of measuring all of the PNMS matrix elements in this single experiment.

A highly-capable near detector is needed to provide precision measurements of the unoscillated flux spectrum, and precisely measure neutrino cross-sections

necessary to interpret the far detector signal and backgrounds. Such a detector will also have a significant physics program in its own right addressing many non-oscillation topics such as neutrino cross-sections, precision electroweak measurements and searches for new physics.

Due to the underground location of the detector, the physics reach of this program extends well beyond the beam oscillation measurements. Some prominent examples of the broad non-accelerator physics program enabled by a large underground liquid argon detector include: baryon-number-violating decay searches with unprecedented reach, collection of an exquisitely-reconstructed sample of atmospheric neutrinos, which can be used to enhance oscillation studies, and unique, high-statistics detection of the electron-neutrino component of a Milky-Way core-collapse supernova neutrino burst, which will reveal otherwise-invisible physics and astrophysics.

2.0 Physics Program

2.1 Long-Baseline Neutrino Oscillation Physics

2.1.1 Phenomenology

To first order, the oscillation probability of $\nu_\mu \rightarrow \nu_e$ through matter in a constant density approximation is [1]:

$$P(\nu_\mu \rightarrow \nu_e) \simeq \sin^2\Theta_{23}\sin^2 2\Theta_{13}\frac{\sin^2(\Delta_{31}-aL)}{(\Delta_{31}-aL)^2}\Delta_{31}^2 \quad (1)$$

$$+\sin 2\Theta_{23}\sin 2\Theta_{13}\sin 2\Theta_{12}\frac{\sin(\Delta_{31}-aL)}{(\Delta_{31}-aL)}\Delta_{31}\frac{\sin(aL)}{(aL)}\Delta_{21}\cos(\Delta_{31}+\delta_{CP})$$

$$+\cos^2\Theta_{23}\sin^2 2\Theta_{12}\frac{\sin^2(aL)}{(aL)^2}\Delta_{21}^2,$$

where,

$$\Delta_{ij} = \Delta m_{ij}^2 L/4E, \text{ and } a = G_F N_e/\sqrt{2}.$$

In the above, both δ_{CP} and a switch signs in going from the $\nu_\mu \rightarrow \nu_e$ to the $\overline{\nu}_\mu \rightarrow \overline{\nu}_e$ channel; i.e., a neutrino-antineutrino asymmetry is introduced both by the CP-violating phase, δ_{CP}, and the matter effect, the origin of which is simply the presence of electrons and absence of positrons in the Earth. The asymmetry from the matter effect depends on the sign of Δm_{32}^2 and increases with baseline as the neutrinos pass through more matter, so an experiment with a longer baseline will

be more sensitive to the neutrino mass hierarchy. For baselines longer than ~1200 km, the degeneracy between the asymmetries from matter and CP-violation effects can be resolved, so the Fermilab LBNF, with a baseline of 1300 km, will be able to determine the neutrino mass hierarchy unambiguously and measure the value of δ_{CP} in the same experiment.

The electron neutrino appearance probability, $P(\nu_\mu \rightarrow \nu_e)$ is shown in Figure 1 at a baseline of 1300 km as a function of neutrino energy for several values of δ_{CP}. As this figure illustrates, the value of δ_{CP} affects both the amplitude and frequency of the oscillation. The difference in probability amplitude for differing values of δ_{CP} is larger at higher oscillation nodes, which here correspond to energies less than 1.5 GeV. Therefore, it is desirable to have a broadband experiment capable of measuring not only the rate of ν_e appearance but also of mapping out the spectrum of observed oscillations down to energies of at least 500 MeV. Since there are terms proportional to sin δ_{CP} in Eq. 1, changes to the value of δ_{CP} induce opposite changes to ν_e and $\overline{\nu}_e$ appearance probabilities, so a beam that is capable of operating in neutrino (forward horn current) and antineutrino (reverse horn current) is also a critical component of the experiment.

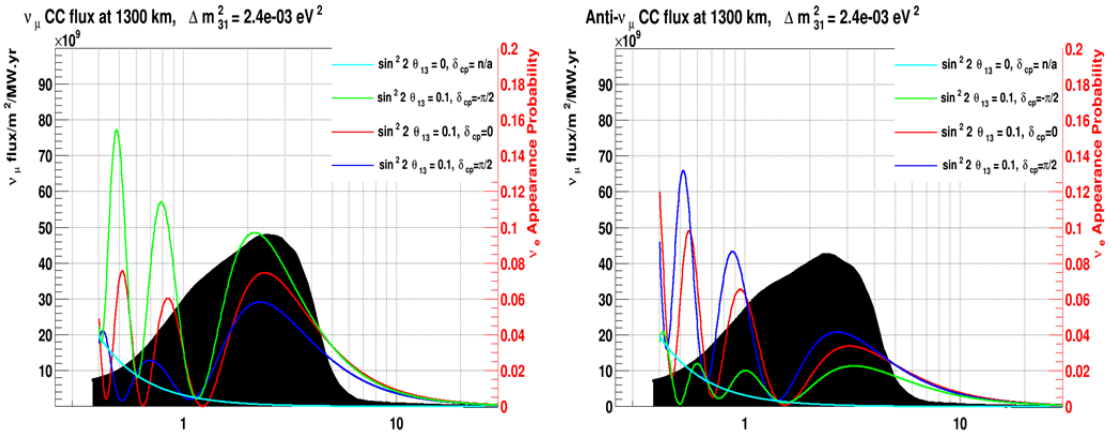

Figure 1: The colored curves represent $P(\nu_\mu \rightarrow \nu_e)$ at a baseline of 1300 km, as a function of neutrino energy, for δ_{CP} = π/2 (blue), 0 (red), and -π/2 (green), for neutrinos (left) and antineutrinos (right), for normal hierarchy. The cyan curve indicates the oscillation probability if θ_{13} were equal to zero. The black solid histogram is the unoscillated ν_μ (left) and $\bar{\nu}_\mu$ (right) flux at 1300 km from an 80GeV MI beam using NuMI horns for focusing .

Figure 2 shows the expected event rate, calculated from expected flux, cross-section, and oscillation probabilities, as a function of neutrino energy for a 40-kt fiducial mass LAr TPC at a baseline of 1300 km, assuming a perfect focus, 60-GeV beam from Fermilab. The perfect focus beam is described in Section 2.1.3; it is important to note that the background from neutral current and ν_τ interactions is

larger in the perfect focus than in a realistic beam because the perfect focus beam includes a large high-energy tail. As illustrated in Fig. 2, it is possible to collect a large sample of ν_e appearance and ν_μ disappearance events covering a broad range of energies with significant statistics at the energy of the second oscillation maximum. The maximum power available from the Fermilab accelerator complex is dependent on the proton beam energy and the actual flux will depend on details of the hadron production process and the focusing design; optimization of the beam design to maximize experimental sensitivity is a critical aspect of the experiment design and will be discussed further in Section 2.1.3.

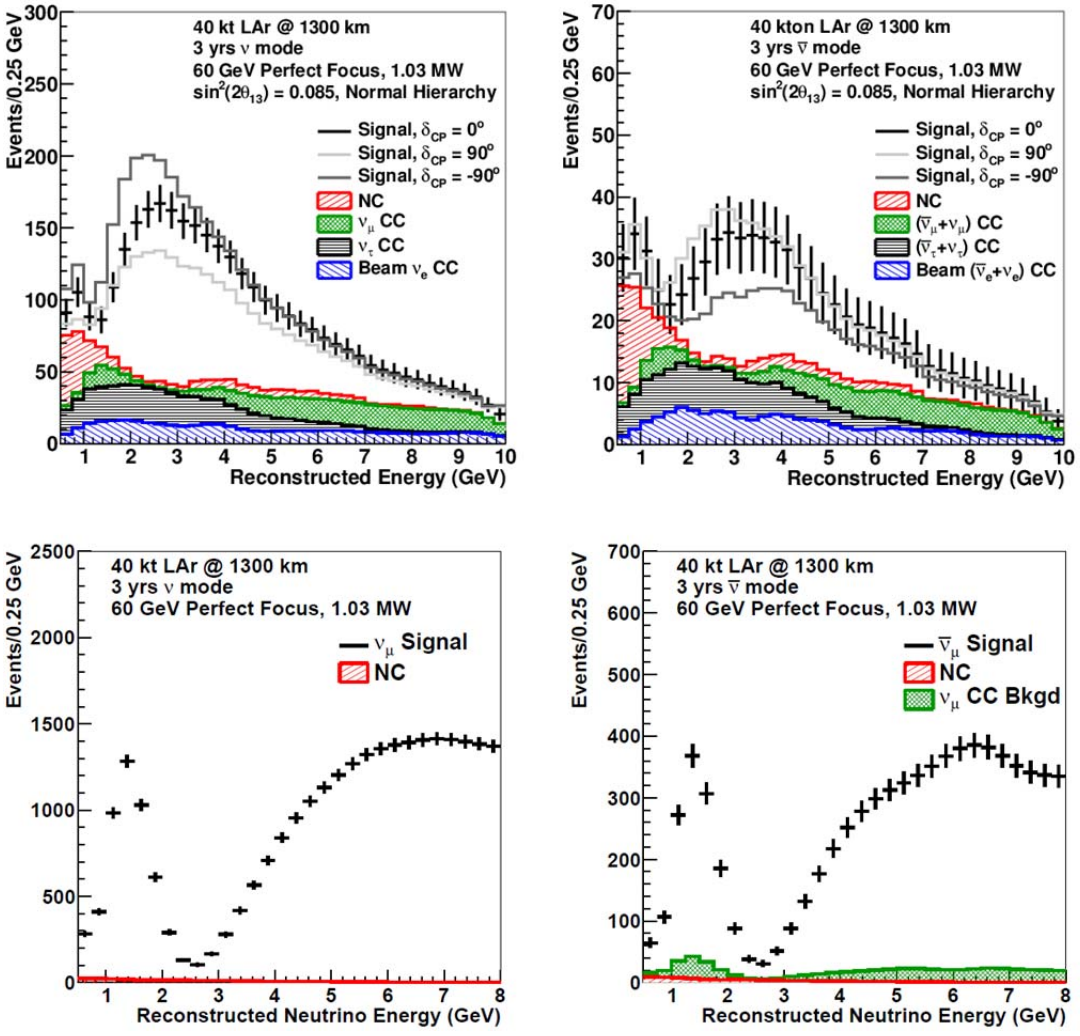

Figure 2: The expected reconstructed neutrino energy spectrum of ν_e appearance (top) and ν_μ disappearance (bottom) events in a 40-kt fiducial mass LArTPC for three years of neutrino (left) and three years of antineutrino (right) running with a 1.03-MW, 60-GeV perfect focus beam. The number of expected signal plus background events is shown for δ_{CP} = -π/2, 0, and π/2. Spectra are for normal hierarchy.

2.1.2 Mass Hierarchy and CP Violation Sensitivities

The experimental sensitivities presented here are estimated using the GLoBES[2, 3] package. GLoBES takes user-provided flux simulation, cross-sections, and detector-response parameterization as inputs. In this document we consider experimental performance for four beams that are labeled according to the proton energy of the primary beam: 120-GeV horn focused, 120-GeV perfect focus, 80-GeV horn focused, and 60-GeV perfect focus. These beams are chosen to demonstrate the possible range of sensitivity, with the perfect focus beams illustrating a more ideal case, though it is important to note that because of their high-energy tails, perfect focus beams are not perfectly optimized beams for the measurements proposed here. The beam power available from the FNAL beam complex varies with proton beam energy, so different power is used in association with each beam energy. The four example beams are described in some detail in Section 2.1.3. The cross-section inputs to GLoBES have been generated using GENIE.

The LAr TPC performance parameters that go into the GLoBES calculation have been described in detail in [4]. The detector configuration used for these studies is referred to as ELBNF as shorthand for experimental program at the Fermilab long-baseline neutrino facility. The detector response assumed in these calculations is summarized in Table 1. The smearing and misidentification rates for the ν_τ

Table 1: LArTPC detector performance parameters assumed in GLoBES sensitivity calculations. Signal efficiencies, background levels, and resolutions are obtained from ICARUS results and LArSoft simulations.

Parameter	Value Used for the ELBNF Sensitivities
	For ν_e CC appearance studies:
ν_e CC efficiency	80%
ν_μ NC mis-identification rate	1%
ν_μ CC mis-identification rate	1%
	For ν_μ CC disappearance studies:
ν_μ CC efficiency	85%
ν_μ NC mis-identification rate	1%
Other background	0%
	Neutrino energy resolutions:
ν_e CC energy resolution	$15\%/\sqrt{E(GeV)}$
ν_μ CC energy resolution	$15\%/\sqrt{E(GeV)}$

Table 2: Central value and relative uncertainty of neutrino oscillation parameters from a global fit to neutrino oscillation data, for normal hierarchy. The relative uncertainty is computed using 1/6 of the 3σ allowed range from the fit.

Parameter	Central Value	Relative Uncertainty
Θ_{12}	0.5843	2.3%
Θ_{23}	0.738	5.9%
Θ_{13}	0.148	2.5%
Δm^2_{21}	7.5×10^{-5} eV^2	2.4%
Δm^2_{31}	2.457×10^{-3} eV^2	2.0%

background vary with energy; these parameters are taken from GENIE simulations. The neutrino oscillation parameters and the uncertainty on those parameters are taken from the Nu-Fit[5] global fit to neutrino data; the values are given in Table 2.

Sensitivity to determination of the neutrino mass hierarchy and discovery of CP violation are obtained by simultaneously fitting the $\nu_\mu \rightarrow \nu_\mu$, $\overline{\nu}_\mu \rightarrow \overline{\nu}_\mu$, $\nu_\mu \rightarrow \nu_e$, and $\overline{\nu}_\mu \rightarrow \overline{\nu}_e$ oscillated spectra. An example of the ν_e appearance and ν_μ disappearance spectra is shown in Fig. 2. The background to ν_e appearance is composed of: i) intrinsic ν_e and $\overline{\nu}_e$ from the beam; ii) mis-identified ν_μ and $\overline{\nu}_\mu$ CC events; iii) neutral current (NC) backgrounds; iv) ν_τ and $\overline{\nu}_\tau$ CC events in which the τ's decay leptonically into electrons/positrons. NC and ν_τ backgrounds are due to interactions of higher energy neutrinos but they contribute to backgrounds mainly at low energy, which is important for the sensitivity to CP violation. Compared to the number of events shown in Figure 2, an optimization of the beam, reducing the high-energy tail of the flux, will help in significantly reducing this background. As shown in [6], ν_τ interactions have a different energy-missing momentum distribution compared to the signal events and with appropriate cuts, not yet included in this analysis, this background can be significantly reduced.

The neutrino oscillation parameters are all allowed to vary, constrained by a Gaussian prior with 1σ width given by the relative uncertainties shown in Table 2. The effect of systematic uncertainty is approximated using signal and background normalization uncertainties, which are treated as 100% uncorrelated among the four samples. Unless otherwise stated, the goal uncertainties of 1% on signal normalization and 5% on background normalization for the ν_e and $\overline{\nu}_e$ appearance measurements, in conjunction with uncorrelated 5% signal and 10% background normalization uncertainties in the ν_μ and $\overline{\nu}_\mu$ disappearance measurements, are

used to calculate the sensitivities. Further discussion of systematic uncertainty, including a preliminary justification of these values and the effect of considering larger signal and background normalization uncertainties, is presented in Section 2.1.4.

In these fits, experimental sensitivity is quantified using a test statistic, $\Delta\chi^2$, which is calculated by comparing the predicted spectra for alternate hypotheses. These quantities are defined, differently for neutrino mass hierarchy and CP violation sensitivity, to be:

$$\Delta\chi^2_{\mathrm{MH}} = \chi^2_{\mathrm{IH}} - \chi^2_{\mathrm{NH}} \text{ (true normal hierarchy)}$$

$$\Delta\chi^2_{\mathrm{MH}} = \chi^2_{\mathrm{NH}} - \chi^2_{\mathrm{IH}} \text{ (true inverted hierarchy)} \quad (2)$$

$$\Delta\chi^2_{\mathrm{CPV}} = \min[\Delta\chi^2_{\mathrm{CP}}(\delta^{\mathrm{test}}_{\mathrm{CP}} = 0), \Delta\chi^2_{\mathrm{CP}}(\delta^{\mathrm{test}}_{\mathrm{CP}} = \pi)], \text{ where} \quad (3)$$

$$\Delta\chi^2_{\mathrm{CP}} = \chi^2_{\delta^{\mathrm{test}}_{\mathrm{CP}}} - \chi^2_{\delta^{\mathrm{true}}_{\mathrm{CP}}} \quad (4)$$

Since the true value of δ_{CP} is unknown, a scan is performed over all possible values of $\delta^{\mathrm{true}}_{\mathrm{CP}}$. We define a "typical experiment" as one with the most probable data given a set of input parameters, i.e. in which no statistical fluctuations have been applied. In this case, the predicted spectra and the true spectra are identical; for the example of CP violation, $\chi^2_{\delta^{\mathrm{true}}_{\mathrm{CP}}}$ is identically zero and the $\Delta\chi^2_{\mathrm{CP}}$ value for a typical experiment is given by $\chi^2_{\delta^{\mathrm{test}}_{\mathrm{CP}}}$.

The expected sensitivity of this experiment to determination of the neutrino mass hierarchy and CP violation are shown in Fig. 3. These calculations are for a 40-kt fiducial mass detector operating for three years in neutrino mode and three years in antineutrino mode, with an 80-GeV beam from FNAL using NuMI-style focusing. The results are shown as a function of the true value of δ_{CP} for the range of true values of θ_{23} allowed by the current global fit. The number of events expected in each mode are shown in Table 3.

The value of the test statistic for a typical experiment, $\overline{\Delta\chi^2}$, is representative of the mean or the most likely value of $\Delta\chi^2$ that would be obtained in an ensemble of experiments. With the exception of Figure 4, the sensitivity plots in this document have been generated using this method. However, to address the expected sensitivity of a future experiment requires consideration of the effect of statistical fluctuations and variations in systematics. If the experiment is repeated many times, a distribution of $\Delta\chi^2$ values will appear. Studies in [7, 8] show that, in the

case of the mass hierarchy determination, the $\Delta\chi^2$ metric *does not* follow the commonly expected chi-squared function for one degree of freedom, which has a mean of $\overline{\Delta\chi^2}$ and can be interpreted using a Gaussian distribution with a standard deviation of $\sqrt{|\overline{\Delta\chi^2}|}$. Rather, these studies show that when the observed counts in the experiment are large enough, the distribution of $\Delta\chi^2$ used here approximately follows a Gaussian distribution with a mean and standard deviation of $\overline{\Delta\chi^2}$ and $\sqrt{|\overline{\Delta\chi^2}|}$, respectively. Figure 4 shows the range of sensitivity to the neutrino mass hierarchy, for the nominal exposure of 257 kt-MW-years, when statistical fluctuations are included and the statistical power as a function of exposure for 3σ and 5σ sensitivity.

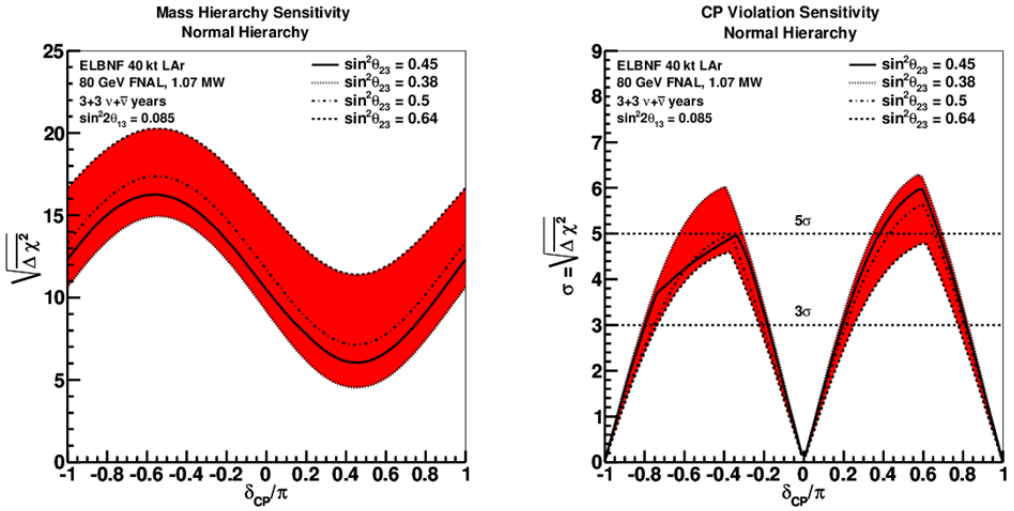

Figure 3: Expected sensitivity of ELBNF to determination of the neutrino mass hierarchy (left) and discovery of CP violation, i.e. $\delta_{CP} \neq 0$ or π, (right) for a 40-kt fiducial mass LAr TPC and an 80-GeV, 1.07-MW beam from FNAL to SURF with three years of running in neutrino and three years in antineutrino mode. The Nu-Fit central value for θ_{23} (solid line) is shown in comparison with other values of θ_{23} The width of the band corresponds to the 3σ range allowed by Nu-Fit. Note that the sensitivity to MH increases for increasing values of θ_{23} while the corresponding sensitivity to CP violation decreases. Sensitivities are for true normal hierarchy; neutrino mass hierarchy is assumed to be unknown in the CPV fits.

Table 3: Expected number of ν_e appearance signal and background events in the energy range 0.5-10.0 GeV at the far detector after detector smearing and event selection. The signal events are shown for δ_{CP} = -π/2, 0, and π/2, for a 40-kt fiducial mass LAr TPC and an 80-GeV, 1.07-MW beam from FNAL to SURF with three years of running in neutrino and three years in antineutrino mode. Neutrino and antineutrino events are combined for both signal and background. Normal hierarchy is assumed.

Run Mode	Signal Events δ_{CP}			Background Events			
	$-\pi/2$	0	$\pi/2$	ν_μ NC	ν_μ CC	ν_e Beam	ν_τ CC
Neutrino	1068	864	649	72	83	182	55
Antineutrino	166	213	231	41	42	107	33

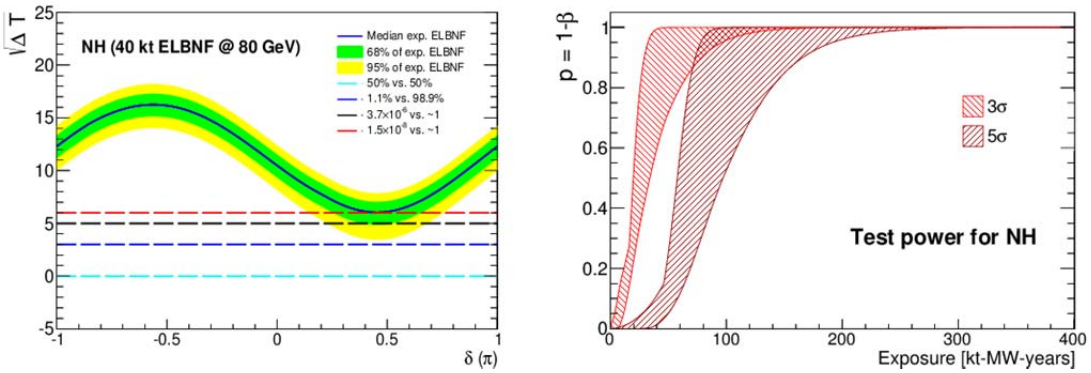

Figure 4: Sensitivity to neutrino mass hierarchy including statistical fluctuations. Expected sensitivity of ELBNF to determination of the neutrino mass hierarchy for a 40-kt fiducial mass LAr TPC and an 80-GeV, 1.07-MW beam from FNAL to SURF with three years of running in neutrino and three years in antineutrino mode. Left: The sensitivity, given by $\sqrt{\Delta T} = \sqrt{\overline{\Delta\chi^2}}$, for a typical experiment (solid blue line) is compared to the bands within which 68% (green) and 95% (yellow) of experiments are expected to fall. The dashed lines represent the value of the ΔT metric above which the minimum probability of determining the correct neutrino mass hierarchy is 50%(cyan), 98.9% (blue), or 1-3.7x10^{-6} (black). The red line shows the minimum sensitivity for a typical experiment. Right: The test power (p=1−β), which represents the probability of accepting the correct (NH) hypothesis, while excluding the incorrect (IH) hypothesis at the 3σ and 5σ level, shown as a function of exposure in kt-MW-years. The width of the bands represent the range of δ_{CP} values. Sensitivities are for true normal hierarchy.

2.1.3 Beam Optimization

The current reference design for the Fermilab-based LBNF neutrino beamline is presented in Section 3.4 below. Active studies described in this section are under way to further optimize this design, and significant improvements in the capabilities for the long-baseline program appear feasible.

The LBNF neutrino beam is driven by the 120 GeV Fermilab Main Injector. Proton beam energies lower than 120 GeV may be desirable for long-baseline neutrino experiments because they produce more neutrino flux at lower energies and produce less background from higher-energy neutrino interactions, facilitating spectral analysis covering a wider range of energy. A planned upgrade to the FNAL accelerator complex (PIP-II) [9] will provide 1.2 MW of 120-GeV protons as well as flexibility to provide significant beam power at lower energies. The beam power expected for energies in the 60-120 GeV range is shown in Table 4; these values for beam power are included in the sensitivity calculations in this document.

Table 4: Beam power expected from the FNAL accelerator complex after the PIP-II upgrade for several values of proton energy.

Beam Energy (GeV)	Power (MW)
60	1.03
80	1.07
120	1.20

A comparison of the unoscillated flux from the four example beams considered in this document is shown in the left panel of Fig. 5. The "perfect focus" beams assume perfect hadron focusing and a decay pipe that is 4 m in diameter and 380 m long. Note that this is for illustration only; constraints from the FNAL site limit the actual length of the decay pipe to 250 m. The flux for the two "FNAL-NuMI" beams is from GEANT-based simulations of a NuMI-like beam line. The 120-GeV beam is described in the LBNE CDR[10]: a ~1-m graphite target, a focusing system consisting of two parabolic horns operating at 200 kA, and an air-filled decay pipe that is 4 m in diameter and 200 m long. Since the writing of the CDR, it has been demonstrated that the horn current can be increased to 230 kA and the design for the decay pipe system has been changed to replace the air fill described in [10] with helium.

The beam energy is tunable by adjusting the distance from the target to the upstream face of the first focusing horn; in the nominal design this distance is

35 cm. The 80-GeV beam is also based on the NuMI design but includes a number of upgrades relative to the 120-GeV beam to increase the neutrino flux in the desired energy range. These changes are an upgrade to the target composition, increased horn current to 230 kA, and a helium-filled decay pipe that is 6 m in diameter and 250 m long. The flux increase from each of these changes is given in Table 5 for energy ranges roughly corresponding to the first and second oscillation maxima. Figure 6 shows the sensitivity to mass hierarchy and CP violation for these four example beams.

The right panel of Fig. 5 shows a comparison between the 120-GeV FNAL beam and a preliminary attempt at optimization, which has been done using a genetic algorithm that maximizes estimated sensitivity to δ_{CP}. This optimization is similar

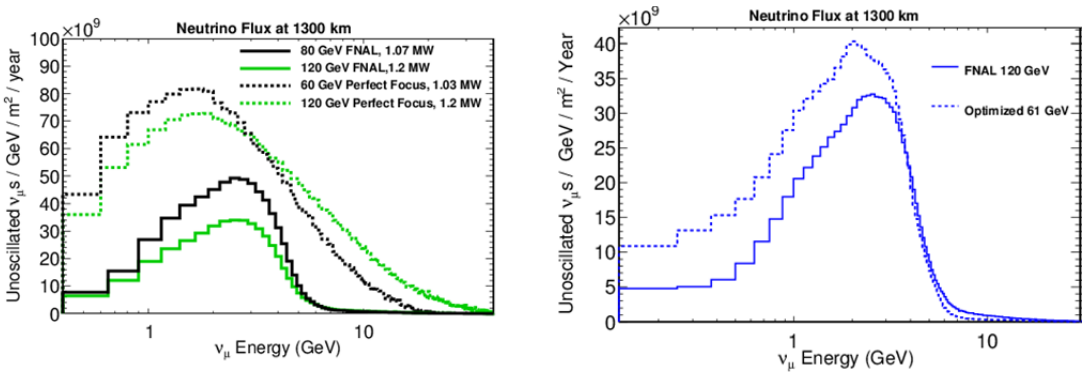

Figure 5: Unoscillated ν_μ flux at 1300 km in units of neutrinos per GeV per square meter per year. The left panel shows the flux for the four beams described in the text: 120-GeV FNAL (solid green), 80-GeV FNAL (solid black), 120-GeV perfect focus (dashed green), and 60-GeV perfect focus (dashed black). The right panel shows the flux resulting from a preliminary attempt at further beam optimization (dashed) compared to the 120-GeV FNAL beam (solid). In all cases, the variation in beam power with proton beam energy is considered in the normalization.

Table 5: Increase in neutrino flux relative to the 120-GeV FNAL beam in the energy ranges 0.5-2 GeV and 2-5 GeV for each upgraded design feature in the 80-GeV FNAL beam.

Design Change	Flux Increase 0.5-2 GeV	Flux Increase 2-5 GeV
Target: NuMI graphite → Be cylinder	1.10	1.00
Horn current: 200 kA → 230 kA	1.00	1.12
Decay pipe: Air → He	1.07	1.11
Decay pipe diameter: 4 m → 6 m	1.06	1.02
Decay pipe length: 200 m → 250 m	1.04	1.12

to one done as part of the LAGUNA-LBNO design study[11] and yields horn shapes similar to those optimized for a 50 GeV high-power PS at CERN, which is illustrated in Fig. 4.12 of [11]. Within this optimization, parameters such as primary proton momentum, target dimensions, and horn shape are varied. The best configuration found by the algorithm produces a muon neutrino flux that is 20% greater than the nominal configuration at the first oscillation maximum, 50% greater at the second oscillation maximum, and reduces the antineutrino contamination of the beam. It is expected that the optimized beam will lead to improvements in sensitivity to both mass hierarchy and CP violation. Refinement of the optimization procedure, quantification of the sensitivity improvement, and evaluation of the feasibility of the optimized designs are in progress.

The sensitivities for the perfect focus beams set the scale of improvement that is possible from optimization of the focusing system for the neutrino beam. As seen in Fig. 6, the most dramatic improvements are for mass hierarchy sensitivity in the

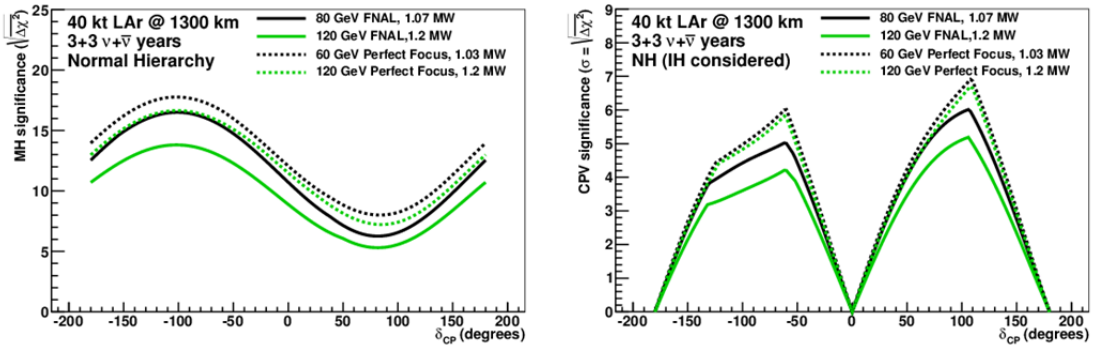

Figure 6: Expected sensitivity of the experiment to determination of the neutrino mass hierarchy (left) and discovery of CP violation, i.e. $\delta_{CP} \neq 0$ or π, (right). Sensitivities are shown for a 40-kt fiducial mass LAr TPC, with three years of running in neutrino and three years in antineutrino mode, for four example neutrino beams, 120-GeV and 80-GeV beams with NuMI-style focusing (solid lines) and 120-GeV and 60-GeV perfect focus beams (dashed lines), details of which are described in the text. Sensitivities are for true normal hierarchy; neutrino mass hierarchy is assumed to be unknown in the CPV fits.

region near $\delta_{CP} = \pi/2$, where additional events from the second oscillation maximum help to break the near-degeneracy between the CP and matter asymmetries. Sensitivity to CP violation also has significant room for improvement. As illustrated in Fig. 7, which shows the sensitivity as a function of exposure for the 120-GeV FNAL beam and the 60-GeV perfect focus beam, which are expected to span the range of potential beam performance, optimization of the beam design will allow discovery-level sensitivity to be reached with significantly lower exposure, making this optimization a crucial feature of the experiment design.

2.1.4 Systematic Uncertainties

As described in Section 2.1.2, the effect of systematic uncertainty on experimental sensitivity is approximated using signal and background normalization uncertainties. In the sensitivities presented here, the normalization uncertainties on the ν_μ and $\overline{\nu}_\mu$ samples are 5% on signal and 10% on background. In this section, we consider the effect of varying the size of the residual normalization uncertainties on the ν_e and $\overline{\nu}_e$ samples, which are 100% uncorrelated from each other and from the ν_μ and $\overline{\nu}_\mu$ uncertainties. Figure 8 shows the sensitivity to neutrino mass hierarchy and discovery of CP violation as a function of exposure for several levels of this uncertainty.

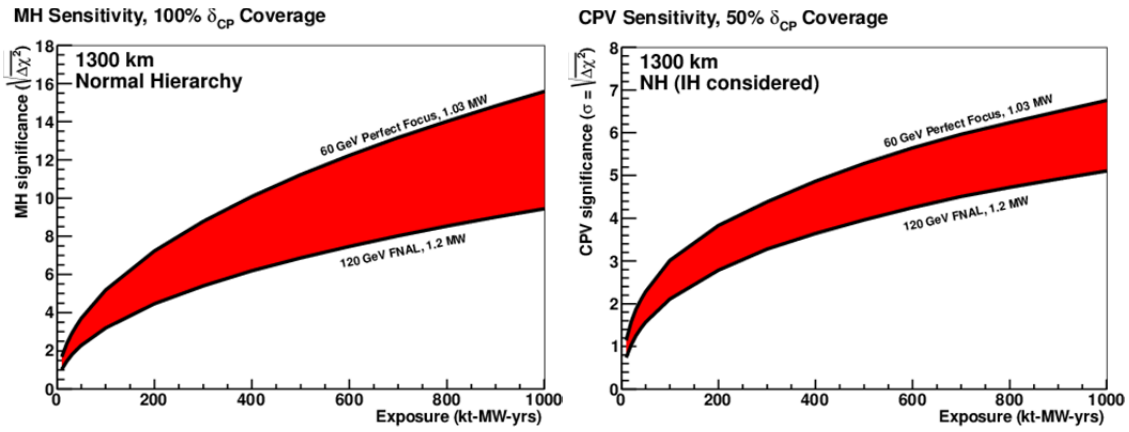

Figure 7: Expected sensitivity of the experiment to determination of the neutrino mass hierarchy (left) and discovery of CP violation, i.e. $\delta_{CP} \neq 0$ or π, (right) as a function of exposure in kt-MW-years, assuming equal running in neutrino and antineutrino mode, for neutrino beams ranging from the 120-GeV beam with NuMI-style focusing to the 60-GeV perfect focus beam, details of which are described in the text. The sensitivities quoted are the minimum sensitivity for 100% of δ_{CP} values in the case of mass hierarchy and 50% of δ_{CP} values in the case of CP violation. Sensitivities are for true normal hierarchy; neutrino mass hierarchy is assumed to be unknown in the CPV fits.

As seen in Fig. 8, for early phases with exposures less than 100 kt-MW-years, the experiment will be statistically limited. In the full experiment, signal and background normalization uncertainties remain relatively unimportant for the mass hierarchy measurement, when considering minimum sensitivity for 100% of δ_{CP} values, because the minimum sensitivity occurs in the near-degenerate region where δ_{CP} is near $\pi/2$. In this region, much of the sensitivity to mass hierarchy comes from spectral analysis of the oscillations and is therefore less sensitive to

normalization uncertainty. It is important to note that the sensitivity calculations presented here do not consider the effect of energy scale uncertainty, which may have a more significant impact on mass hierarchy sensitivity. Studies of the impact of energy scale uncertainty are in progress and will be included in future analyses of experimental sensitivity.

The impact of systematic uncertainty on the CP violation sensitivity is obvious in Fig. 8; the normalization of the ν_e sample, relative to the $\bar{\nu}_e$, ν_μ, and $\bar{\nu}_\mu$ samples after all constraints from external, near detector, and far detector data have been applied, must be determined at the 1-2% level in order to reach 5σ sensitivity for exposures less than 900 kt-MW-years.

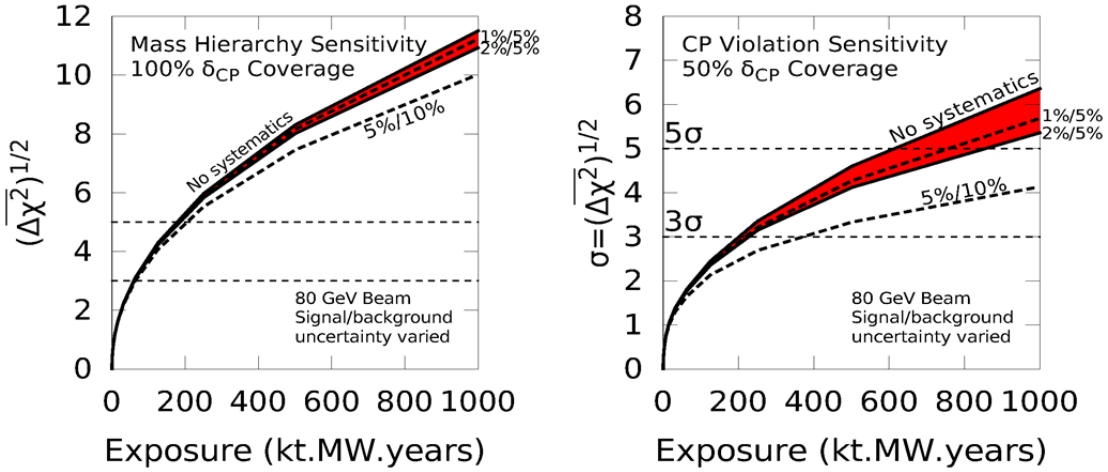

Figure 8: Expected sensitivity of ELBNF to determination of the neutrino mass hierarchy (left) and discovery of CP violation, i.e. $\delta_{CP} \neq 0$ or π, (right) as a function of exposure in kt-MW-years, assuming equal running in neutrino and antineutrino mode, for a range of values for the residual ν_e and $\bar{\nu}_e$ signal and background normalization uncertainties. The sensitivities quoted are the minimum sensitivity for 100% of δ_{CP} values in the case of mass hierarchy and 50% of δ_{CP} values in the case of CP violation. Sensitivities are for true normal hierarchy; neutrino mass hierarchy is assumed to be unknown in the CPV fits.

Uncertainties in in the experiment will be constrained by external data, near detector data, and the combined fit to the four (ν_e, $\bar{\nu}_e$, ν_μ, $\bar{\nu}_\mu$) far detector samples. Experience from previous and currently-running neutrino oscillation experiments suggests that 1-2% uncertainty in uncorrelated ν_e signal normalization and 5% uncorrelated uncertainty in background normalization for the ν_e -appearance measurement is reasonably achievable if the experiment has a capable near detector. Table 6 shows the uncertainties in a ν_e appearance analysis achieved by MINOS [12] and T2K [13] and compares the expected uncertainty in the proposed experiment. The projected uncertainties in the proposed experiment are chosen by

determining which of the existing experiments is more representative of the proposed experiment for each source of systematic uncertainty and then setting the reasonable goal that a next generation experiment, with the high resolution of a LArTPC and precise measurements from a highly capable near detector, should be able to improve on a similar earlier experiment. Based on this exercise, the *total* uncertainty on the ν_e sample is expected to be less than 4%; significant cancellation of uncertainty is expected in the four-sample fit, so the residual uncorrelated uncertainty is expected to be reduced to the 1-2% level.

Better determination of expected systematic uncertainty using more sophisticated simulations and tools is a high priority of the collaboration and is in progress. Detailed description of this effort is beyond the scope of this document; only a brief summary of preliminary results will be presented here.

Initial studies using a Fast Monte Carlo with a parameterized near detector response predict 2-3% statistical uncertainties on the absolute flux using fully leptonic neutrino interactions for which high-precision cross-section predictions exist. Specifically, the statistical uncertainty is expected to be 2% for neutrino-electron scattering (E_ν <5 GeV) and 3% for inverse muon decay (E_ν >11 GeV). Relative normalization using the low-ν_0 method is expected to constrain the flux shape and the near/far flux ratio to 1-2%. Studies using a multi-sample fit to constrain the flux with simulated near detector event samples show significant constraints on all flux uncertainties. The post-fit uncertainty in most flux bins for a preliminary fit is less than 5%, which is the uncorrelated ν_μ signal normalization uncertainty assumed by the sensitivity calculations.

Uncertainty from nuclear interactions, in which particles exiting the primary interaction vertex interact with the nuclear medium prior to depositing energy in the detector, and detector effects, such as resolutions and energy scale uncertainty, are somewhat more difficult to address with early simulation efforts. However, in analogy to the treatment of cross-section uncertainty described above, the effect of varying nuclear interaction parameters within their GENIE uncertainties and comparisons of GENIE predictions to those of other event generators are in progress. Efforts to improve modeling of nuclear interactions and to develop reconstruction and analysis tools for a full Monte Carlo simulation are also underway. At the same time, a number of test-beam and prototype experiments, including the LBNE 35-t prototype, LARIAT, CAPTAIN, and the CERN neutrino platform experiments, are being designed and built to reduce these uncertainties with experimental data. In addition, the Fermilab short baseline program, including the MicroBooNE, LAr1-ND, and ICARUS experiments, will provide high statistics, precision neutrino cross section measurements, beyond their planned short baseline oscillation goals.

Table 6: The dominant systematic uncertainties on the ν_e-appearance signal prediction in MINOS and T2K and a conservative projection of the expected uncertainties in ELBNF. In each case, the quoted uncertainty is the effect on the ν_e-appearance signal only. These uncertainties are the total expected uncertainties on the ν_e-appearance signal which include both correlated and uncorrelated uncertainties in the three-flavor fit

Source of Uncertainty	MINOS ν_e	T2K ν_e	ELBNF ν_e	Comments
Beam Flux after N/F extrapolation	0.3%	2.9%	2%	MINOS is normalization only. ELBNF normalization and shape highly correlated between ν_μ/ν_e.
Neutrino interaction modeling				
Simulation includes: Hadronization Cross sections Nuclear models	2.7%	7.5%	~2%	Hadronization models are better constrained in the ELBNF LArTPC. N/F cancellation is larger in MINOS/ELBNF. Cross -section uncertainties are larger at T2K energies. Spectral analysis in ELBNF provides extra constraint.
Detector effects				
Energy scale (ν_μ)	3.5%	included above	(2%)	Included in ELBNF ν_μ sample uncertainty only in 3-flavor fit. MINOS dominated by hadronic scale.
Energy scale (ν_e)	2.7%	3.4% includes all FD effects	2%	Totally active LArTPC with calibration and test beam data lowers uncertainty.
Fiducial volume	2.4%	1%	1%	Larger detectors = smaller uncertainty.
Total	5.7%	8.8%	3.6 %	Uncorrelated ν_e uncertainty in full ELBNF 3-flavor fit = 1-2%.

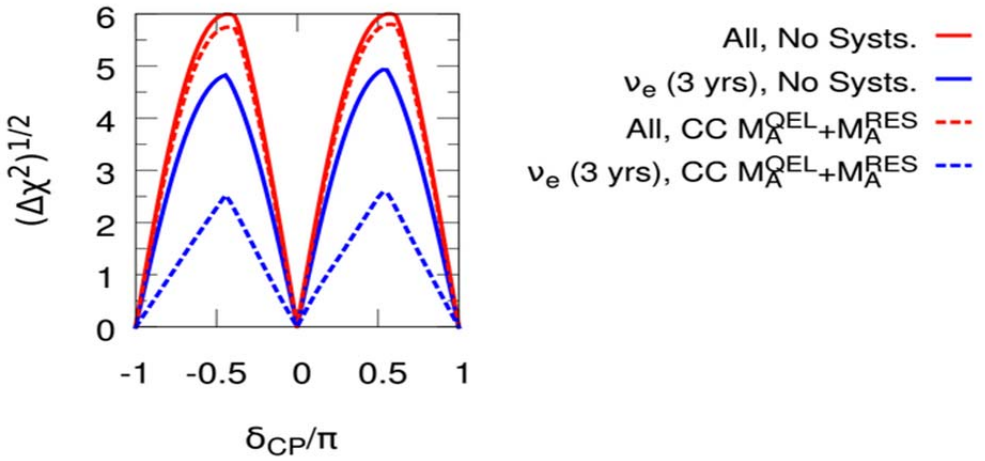

Figure 9: An example CP violation sensitivity calculated using inputs from the FastMC in a fit to all four (ν_e, $\bar{\nu}_e$, ν_μ, $\bar{\nu}_\mu$) samples (red) and a fit to the ν_e appearance sample only (blue), for the case of no systematic uncertainty (solid) and the case in which both $M_A^{QE,CC}$ and $M_A^{RES,CC}$ are allowed to vary with a 1σ uncertainty of 20% (dashed). This example was taken from an earlier LBNE study, so the absolute sensitivity cannot be compared with the sensitivities presented in this document.

2.2 Physics with a Precision Near Detector

To achieve the precision required to make a significant advance in the measurement of neutrino oscillation parameters over current experiments and to reach the desired 5σ sensitivity to CP violation, a highly-capable, high-precision near detector is required to measure the unoscillated flux spectrum to a few percent for all neutrino species in the beam (ν_e, $\bar{\nu}_e$, ν_μ, $\bar{\nu}_\mu$) and to precisely measure neutrino cross sections necessary to interpret the far detector signal and backgrounds. This requires a high resolution, magnetized near neutrino detector for identifying and measuring electrons and muons with high efficiency. To measure both the small ν_e and $\bar{\nu}_e$ contamination in the beam with high precision, the detector would need to be able to distinguish e^+ from e^-; this would require a low-density detector with a commensurately long physical radiation length. Additionally, this would enable a precise determination of the π^0 content in neutrino interactions, which is an important background to the $\nu_e/\bar{\nu}_e$ appearance measurement. Use of a target nucleus similar to the far detector would allow cancellation of systematic errors and inclusion of other target nuclei would provide constraints for accurate modeling of nuclear effects. Such a detector [14] placed in the high-intensity neutrino beam needed for the oscillation measurements will collect a vast sample of neutrino interactions. This will enable a rich program in neutrino scattering physics addressing many non-oscillation topics, such as

neutrino cross sections, precision electroweak measurements and searches for new physics.

2.3 Non-Accelerator Physics

A large liquid argon TPC, when sited underground, has significant capabilities for addressing diverse physics topics, including proton decay, atmospheric and supernova neutrinos. These opportunities are described in detail in [4, 15]. For non-beam physics, no external trigger will be available, and suitable triggering will be required, possibly involving detection of photons produced in the liquid argon by ionizing particles. Table 7 summarizes the expected signal rates. Proton decay and atmospheric neutrino events are, like beam events, GeV scale, and should in principle be quite cleanly identifiable in a LArTPC. Supernova neutrino events have few tens of MeV of energy and will create small lepton tracks involving only a few adjacent channels.

Although these low-energy events may be difficult to discriminate from background, the high-rate pulse of low-energy events all arriving within a roughly 30 seconds interval results in promising signal of the discrete supernova event relative to a well-known continuous background. In contrast, "relic" supernova events arrive singly and the very low expected signal rate will make their selection especially challenging; nevertheless a deep underground location may make the measurement feasible. Solar neutrinos are also a challenging physics target due to the sub-15 MeV energies but, also, may be conceivable to pursue in a low-background underground location.

Table 7: Expected Event Rates for non-accelerator physics signals

Physics	Energy range	Expected signal rate (events $kt^{-1}yr^{-1}$)
Proton decay	~ GeV	< 0.06
Atmospheric neutrinos	0.1–10 GeV	~300
Supernova burst neutrinos	few-50 MeV	~20-100 in 30 s at 10 kpc
Diffuse supernova neutrinos	20-50 MeV	< 0.06
Solar neutrinos	5-15MeV	~3000

2.3.1 Searches for Baryon Number Non-conservation

Baryon number conservation is an unexplained symmetry in the Universe with deep connections to both cosmology and particle physics. As one of the conditions underlying the observed matter-antimatter asymmetry of the Universe, baryon

number should be violated. Nucleon decay, which is a manifestation of baryon number violation, is a hallmark of many Grand Unified Theories (GUTs), theories that connect quarks and leptons in ways not envisioned by the Standard Model. Observation of proton or bound-neutron decay would provide a clear experimental signature of baryon number violation.

The superior detection efficiencies of a large LArTPC for decay modes that produce kaons[16] will significantly outweigh the lower mass compared to proposed multi-100-kt water Cherenkov detectors. Because the LArTPC can reconstruct protons that would otherwise be below Cherenkov threshold, it can reject many atmospheric neutrino background topologies by vetoing on the presence of a recoil proton. Due to its high spatial resolution, it also performs better for event topologies with displaced vertices, such as $p \rightarrow K^+\bar{\nu}$ (for multi-particle K^+ decay topologies) and $p \rightarrow K^0\mu^+$. The latter mode is preferred in some SUSY GUTs.

Figure 10 shows the expected limit as a function of time for $p \rightarrow K^+\bar{\nu}$. According to this plot, approximately 10-kt of LAr will improve the limits significantly beyond current Super-K limits. Other modes for which this technology has an advantages are $n \rightarrow e^-K^+, p \rightarrow K^+\mu^-\pi^+, n \rightarrow e^+\pi^-, p \rightarrow e^+K^0$.

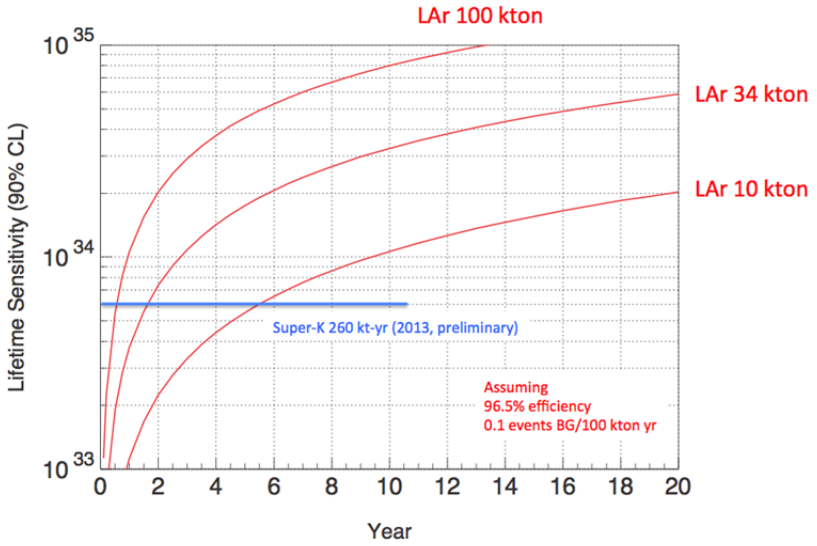

Figure 10: Proton decay lifetime limit for $p \rightarrow K^+\bar{\nu}$ as a function of time for LAr TPC with fiducial masses 10, 34 and 100 kt. For comparison, the current limit from SK is also shown. The limits are at 90% C.L., calculated for a Poisson process including background, assuming that the detected events equal the expected background.

2.3.2 Atmospheric neutrinos:

Atmospheric neutrinos are unique among sources used to study oscillations: the oscillated fluxes contain neutrinos and antineutrinos of all flavors, and matter effects play a significant role. The expected interaction rate is a few hundred events per kt-year, enabling the collection of a large-statistics sample. The excellent CC/NC separation, angular resolution, and the ability to fully reconstruct the hadronic final state in CC and NC interactions, unimpeded by a Cherenkov threshold, will enable the atmospheric neutrino 4-momentum to be fully determined. This will enable a higher-resolution measurement of L/E to be extracted from atmospheric-neutrino events in a LAr TPC compared to the measurements obtained from Super-K.

The atmospheric sample will provide good sensitivity to mass hierarchy (see Figure 11) and to the octant of θ_{23} on its own, and will improve overall sensitivity when combined with accelerator beam measurements. Since the oscillation phenomenology plays out over several decades in energy and path length, atmospheric neutrinos are very sensitive to alternative explanations or subdominant new physics effects that predict something other than the characteristic L/E dependence predicted by oscillations in the presence of matter.

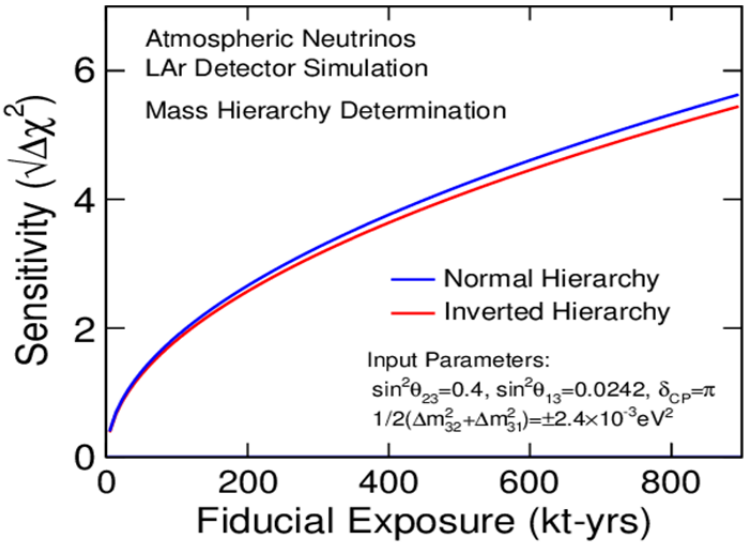

*Figure 11: Sensitivity to mass hierarchy using atmospheric neutrinos as a function of the fiducial exposure in kt*years.*

2.3.3 Core-Collapse Supernova Neutrinos:

A nearby core-collapse supernova will provide a wealth of information via the time, energy and flavor structure of its intense neutrino emission (see [17, 4] for reviews, and references therein). A supernova neutrino burst contains information not only on the astrophysics of the core collapse (e.g. neutronization, black hole formation, shock wave effects, standing accretion shock instability effects, turbulence effects, proto-neutron star cooling) but also on neutrino properties related to neutrino oscillation. A particularly interesting example is the collective effects due to neutrino-neutrino interactions in super-dense matter, which will have observable signatures (see [4] for references) that depend on the neutrino mass hierarchy.

Core-collapse neutrinos are emitted in a burst of a few tens of seconds duration. Energies are in the few tens of MeV range, and luminosity is divided roughly equally between flavors. Ability to measure and tag the different flavor components of the spectrum is essential for extraction of physics and astrophysics from the signal. Currently, world-wide sensitivity is primarily to $\bar{\nu}_e$, via inverse beta decay on free protons, which dominates the interaction rate in water and liquid scintillator detectors. Liquid argon has a unique sensitivity to the *electron flavor* component of the flux, via the absorption interaction on ^{40}Ar, $\nu_e + {}^{40}\mathrm{Ar} \rightarrow e^- + {}^{40}\mathrm{K}^*$. In principle, this interaction can be tagged via the de-excitation gamma cascade although more work needs to be done to understand efficiencies for a given detector configuration. Some thousands of events would be expected in a 40 kt LAr detector for a supernova at 10kpc; estimates vary by model over a fairly wide range. The number of signal events scales with mass and the inverse square of distance as shown in Fig. 12. For a collapse in the Andromeda galaxy, a 40 kt detector would expect just a few events.

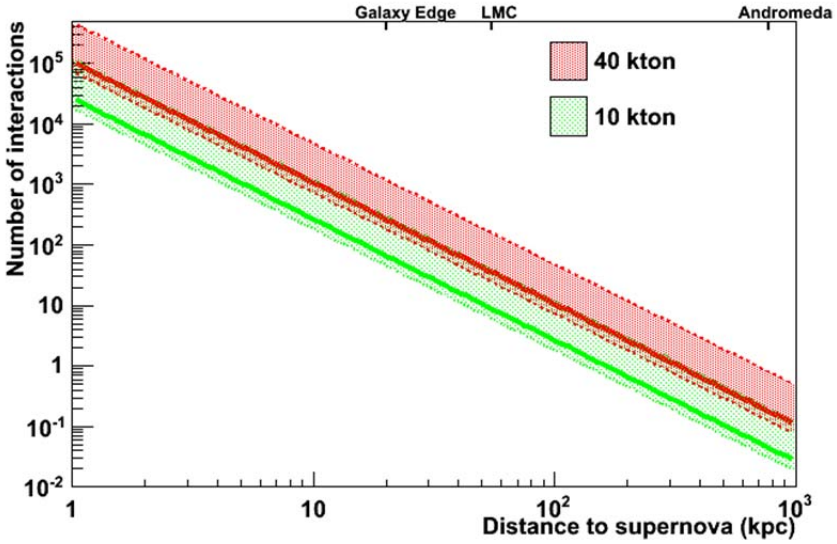

Figure 12: Estimated numbers of supernova neutrino interactions in the experiment as a function of distance to the supernova, for different detector masses (ν_e events dominate). The red dashed lines represent expected events for a 40-kt detector and the green dotted lines represent expected events for a 10-kt detector. The lines limit a fairly wide range of possibilities for "Garching-parameterized" supernova flux spectra (e.g [18]) with luminosity 0.5×10^{52} ergs over ten seconds. The optimistic upper line of a pair gives the number of events for average ν_e energy of $\langle E_{\nu_e} \rangle$ = 12 MeV, and "pinching" parameter α=2; the pessimistic lower line of a pair gives the number of events for $\langle E_{\nu_e} \rangle$ = 8 MeV and α=6. (Note that the luminosity, average energy and pinching parameters will vary over the time frame of the burst, and these estimates assume a constant spectrum. Oscillations will also affect the spectrum.) The solid lines represent the integrated number of events for the specific time-dependent neutrino flux model in [19]. (See Figure 13; this model has relatively cool spectra and low event rates). Core collapses are expected to occur a few times per century in our galaxy, at a most-likely distance of about 10-15 kpc.

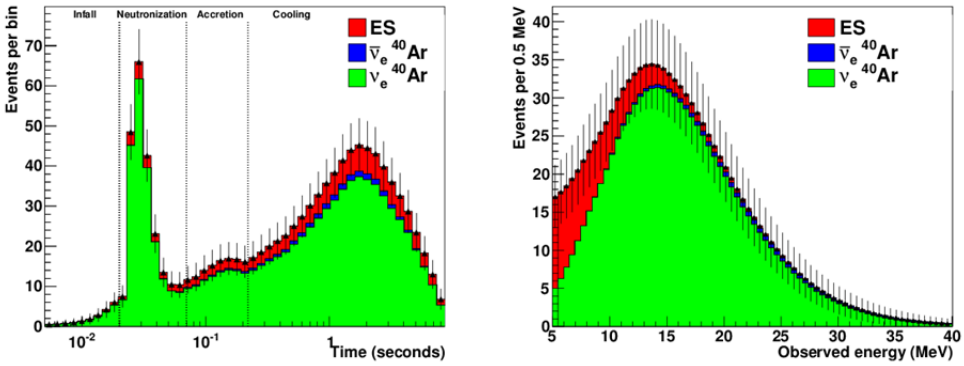

Figure 13: Left: Expected time-dependent signal in 40 kt of liquid argon for a specific flux model for an electron-capture supernova [19] at 10 kpc, calculated using SNoWGLoBES [20]. Note the logarithmic binning in time; the plot shows the number of events expected in the given bin for three detection channels and the error bars are statistical. The vertical dashed line at 0.02 seconds indicates the time of core bounce, and the vertical lines indicate different eras in the supernova evolution. The leftmost time interval indicates the infall period. The next interval, from core bounce to 50 ms, is the neutronization burst era, in which the flux is composed primarily of ν_e. The next period, from 50 to 200 ms, is the accretion period. The final era, from 0.2 to 9 seconds, is the proto-neutron-star cooling period. Right: expected measured event spectrum for the same model, integrated over time.

2.4 The Physics Reach with an Initial 10 kt LAr Detector

A preliminary phase of the experiment, planned to commence data collection in 2021, would use a 10 kt fiducial mass LArTPC and a 700 kW FNAL beam. Here we assume 4 years of data taking, with a neutrino and antineutrino beams or running in neutrinos only. This experimental configuration, with an exposure of 28 MW-kt-yrs and denoted ELBNF28, would be a milestone towards the full experiment. Here we highlight the important physics results that could be obtained both for accelerator neutrinos and for non-accelerator physics from this first module. For the non-accelerator physics the location underground is essential.

2.4.1 Accelerator neutrino physics

The preliminary configuration ELBNF28 will have a significantly smaller number of events compared to the completed experiment, due to the reduced beam power, smaller detector and fewer years of running. In this phase most long-baseline measurements will be strongly statistically limited as can be seen in Table 8 Nevertheless, it will be able to provide some information on the mass ordering and CP violation. It is particularly interesting to consider the case of maximal CP violation as hinted at in the combined analysis of current neutrino oscillation data.

These data show a preference for close-to-maximal CP violation in the negative half: the current best fit values are $\delta = -56^{\circ}$ for Normal Ordering (NO) and $\delta = -106°$ for Inverted Ordering (IO) and the CP conserving values $\delta = 0, \pm\pi$ are excluded at more than 1σ (except for $\delta = \pi$ which is excluded at slightly less than 1σ for IO)[5]. Although these hints of CP violation are not yet statistical significant, it is interesting to consider the physics reach of ELBNF28 if they were to be confirmed, in addition to the general case of $-\pi \leq \delta < \pi$.

Table 8: Expected number of ν_e appearance signal and background events in the energy range 0.5–10.0 GeV at the far detector after detector smearing and event selection. The signal events are shown for $\delta = -\pi/2$, 0, and $\pi/2$, for a 10-kt fiducial mass LAr TPC and an 80-GeV, 700-kW beam from FNAL to SURF with two years of running in neutrino and two years in antineutrino mode. Neutrino and antineutrino events are combined for both signal and background. Normal hierarchy is assumed.

Run Mode	Signal Events δ			Background Events			
	$-\pi/2$	0	$\pi/2$	ν_μ NC	ν_μ CC	ν_e Beam	ν_τ CC
Neutrino	117	94	71	8	9	20	6
Antineutrino	18	23	25	4	5	12	4

Mass ordering.

While at present no information on the mass ordering is available, in the next few years thanks to the 800 km baseline the NOvA experiment will have some sensitivity, which would be improved if combined with T2K results for $\delta < 0$ and Normal Ordering ($\delta > 0$ and Inverted Ordering). A 1300 km baseline will have significantly larger matter effects that help in mass hierarchy determination. Even for the limited exposure of 28 MW-kt-yrs (2 years each of neutrinos and antineutrino running), in the region of maximal CP violation and negative δ, ELBNF28 achieves a median sensitivity of around $\overline{\Delta\chi^2} > 4$, depending on the specific experimental configuration (see Figure 14). The addition of NOvA and T2K data improves the reach in this region of δ slightly and gives a significant contribution for $\delta \geq 0$.

CP-violation determination

Due to the number of events and the large backgrounds at low energy, the sensitivity of ELBNF28 alone to CP violation is comparable to that of NOvA+T2K, reaching 2σ for close-to-maximal CP violation independently from the sign of δ (it should be noted that for $\delta > 0$ NOvA and T2K lose sensitivity due to the mass ordering degeneracy). In this preliminary phase of the experiment, the sensitivity

is strongly determined by the number of events as it can be understood by comparing the lines corresponding to different experimental configurations, 80 GeV versus 120 GeV beams. Systematic errors play a subdominant role as the results are very similar for the two choices of 5%/10% and 1%/5% signal/background normalization uncertainty. Therefore, adding information from NOvA and T2K improves very significantly the physics reach: for maximal CP violation and 2+2 years of neutrino and antineutrino run, nearly 3σ can be reached. This would be a very interesting result that could be confirmed rapidly by the subsequent run of the full experiment with higher power and larger detector. Moreover, at 2σ CP violation could be established for approximately 50% of the values of the δ phase. It should be noted that for the CP violation determination, the combination of neutrino and antineutrinos runs is superior to the one of neutrinos only.

2.4.2 Non-accelerator physics

A 10 kt ELBNF would be the first large-scale and low-threshold LAr detector available in the world and could provide new physics opportunities. Given the size of the detector, an unprecedented sensitivity to proton decay, supernova neutrinos, atmospheric neutrinos would become available.

Baryon Number Violation

As discussed in section 2.3.1, just a 10-kt LAr detector would be able to improve the Super-Kamiokande bound in the $p \to K^+\bar{\nu}$ channel and would provide leading limits on $n \to e^-K^+$, $p \to e^+K^0$, $n \to \mu^+\pi^-$, $p \to \mu^+K^0$, $n \to e^+\pi^-$, for which water Cherenkov detectors have limited reconstruction capabilities.

Core-collapse supernova neutrinos

The detection of supernova neutrinos can shed light on the evolution of these extreme astrophysical environments and on neutrino properties. Currently, most experiments are sensitive only or mainly to the electron antineutrino component of the flux. The 10 kt LAr detector would constitute a step-change in the field, by allowing detection of ν_e via $\nu_e + {}^{40}\mathrm{Ar} \to e + {}^{40}\mathrm{K}^*$. Depending on the supernova model considered, between a few hundred to ~1000 events would be expected for a core-collapse supernova located at 10 kpc from Earth. In Fig. 12 we show the dependence of the number of events on the supernova distance. Uniquely compared to the other flavors, electron neutrinos are emitted early in the supernova evolution in conjunction with the neutronization burst. A supernova burst observation in the 10 kt LAr detector would constitute a prompt supernova alert for astronomers and other detectors. Moreover, combining the information on the neutrino component of the flux with that which can be achieved from water

Cherenkov and liquid scintillator detectors for antineutrinos and the other flavors will play an important role in understanding supernova astrophysics.

Atmospheric neutrinos

The operation of a 10-kt LAr detector for four years would provide around 2000 ν_e CC events for which, even in the sub-GeV energy region, not only the lepton produced in an interaction but also the hadronic products could be reconstructed. These capabilities would be fundamental to developing a detailed understanding of the reconstruction of ν_e CC events and of detector systematics in the GeV range.

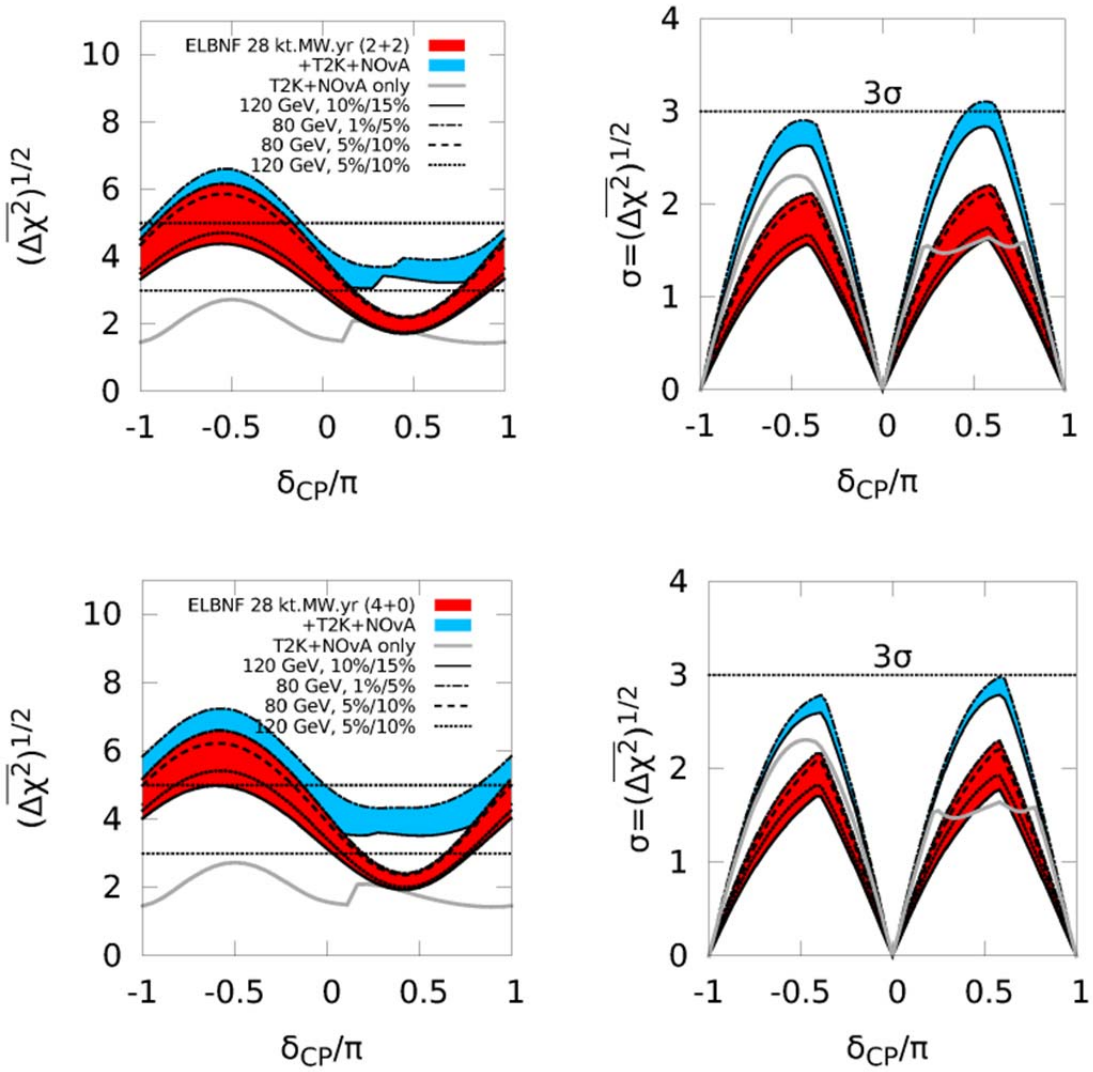

Figure 14: Expected sensitivity of ELBNF28 to the determination of the neutrino mass ordering (left) and discovery of CP violation, i.e. $\delta \neq 0, \pi$, (right), alone (red) and in combination with NOvA and T2K (blue). In the top panels, the ELBNF28 data is divided equally between neutrino and antineutrino mode while for the bottom panels data is in neutrino mode only for the same exposure. Expected sensitivity for a combination of NOvA and T2K without ELBNF28 is indicated by the gray line. The T2K sensitivity is based on 7.8 × 10^{21} protons-on-target (POT) in neutrino mode. The NOvA sensitivity is based on three years of running in neutrino and three years in antineutrino mode, where 6 × 10^{20} POT per year are expected. The systematic uncertainties quoted are the uncorrelated signal/background normalization uncertainties for the ν_e and $\overline{\nu}_e$ samples; each configuration also includes 5%-10% signal/background normalization uncertainty on the muon neutrino and antineutrino samples. The curves on each band represent a range of beam designs and levels of systematic uncertainty, ranging from the 120-GeV FNAL beam with 10%-15% uncertainty to the 80-GeV FNAL beam with 1%-5% uncertainty. Sensitivities are for true normal ordering; neutrino mass ordering is assumed to be unknown in the CPV fits.

3.0 Design of the Experiment

3.1 Overview

To address this broad and exciting physics program, a number of key elements are required:

- A high-intensity, megawatt class, wide-band, sign-selected muon neutrino beam.
- A massive, high-precision neutrino detector, placed deep underground.
- A baseline sufficiently long to determine the mass hierarchy and measure CP-violating effects simultaneously,
- A highly capable precision near detector located close to the neutrino source.

Access to this potentially groundbreaking science is now possible because of the important opportunity provided by the expected availability of a new intense neutrino beam at Fermilab and of underground infrastructures at the Sanford Underground Research Facility, which is at a distance of 1300 km from Fermilab. These facilities will make viable the experimental physics program needed for the elucidation of the fundamental questions described above.

Fermilab is prepared to host the Long-Baseline Neutrino Facility (LBNF), strongly recommended by the P5. As host, Fermilab will provide the infrastructure required to carry out a long-baseline neutrino oscillation experiment with the combination of the required accelerators, beamline, target and horn. The LBNF will include:

- A conventional horn-focused neutrino beam, including a proton transfer line target, horns, decay pipe and absorber, capable of operating at 1.2 MW initially, and with the potential to be upgraded to 2.4 MW. This beam will be driven by the existing Fermilab Main Injector complex, including the planned PIP-II injector upgrades.

- The far site infrastructure with newly expanded underground space at the SURF, which is foreseen to be created after the complete refurbishing of the Ross shaft in 2017 and other site improvements necessary to house the massive LAr-TPC experimental apparatus.

- The near site infrastructure required to house the near detector complex.

- The conventional infrastructure, including the primary technical infrastructure such as the cryostat and associated cryogenics for the liquid argon detector.

To address the groundbreaking physics program made possible by the LBNF, the large international collaboration identified in the author list presented in Appendix A, proposes to construct a deep-underground neutrino observatory based on a 40-kt liquid-argon (LAr) time-projection chamber (TPC) at the Sanford Underground Research Facility. Potential designs for the far detector, using single-phase or dual-phase readout technology, have been developed by a number of groups. These groups have come together to develop an experiment that may employ just one of these technologies, or possibly different technologies in a phased implementation, depending on the performance and developing maturity of the candidate designs. These options are being explored by several groups at the CERN Neutrino Platform (e.g. WA105) as well as Fermilab's short-baseline neutrino program.

The collaboration also proposes to build a fine-grained highly-capable near detector located on the Fermilab site. The reference design of the Near Detector has been developed by the Indian Institutions and Fermilab Collaboration (IIFC) [21], which is an integral part of the LBNE Collaboration. The design consists of a large-volume straw-tube tracking detector and electromagnetic calorimeter inside of a dipole magnet, and resistive plate chambers for muon identification located in the magnet yoke and upstream and downstream steel absorbers. High-pressure argon gas targets and other nuclear targets are embedded in the upstream part of the tracking volume. Alternate designs based on magnetized liquid- or gaseous-argon TPCs have also been proposed, and a modified version of one of these could be integrated into the reference design to enhance the capabilities offered by the fine-grained tracker.

3.2 Liquid Argon Far Detector

We propose to construct a deep-underground neutrino and nucleon decay observatory based on a 40-kt liquid-argon (LAr) time-projection chamber (TPC) [22] at the Sanford Underground Research Facility. The LAr TPC combines fine-grained tracking with total absorption calorimetry to provide a detailed view of particle interactions, making it a powerful tool for neutrino physics and underground physics such as proton decay and supernova-neutrino observation. It provides millimeter-scale resolution in 3D for all charged particles. Particle types can be identified both by their dE/dx and by track patterns, e.g., the decays of stopping particles. The modest radiation length (14 cm) is sufficiently short to identify and contain electromagnetic showers from electrons and photons, but long enough to provide good e/γ separation by dE/dx (one versus two minimum ionizing particles) at the beginning of the shower. In addition, photons can be distinguished from electrons emanating from an event vertex by the flight path

before their first interaction. These characteristics allow the LArTPC to identify and reconstruct signal events with high efficiency while rejecting backgrounds to provide a high-purity data sample.

Potential designs for the far detector have been developed by a number of groups, who now have come together within a single collaboration, including both single-phase and dual-phase readout technology. The far detector may employ just one of these technologies, or possibly different technologies in a phased implementation, depending on the performance and developing maturity of the candidate designs. These options are being explored by several groups at the CERN Neutrino Platform (e.g. WA105[23]) as well as Fermilab's short-baseline neutrino program.

The strategy for integrating these efforts and deciding on the type and configuration of the LBNF far detector system, including the possibility of phased implementation that may involve modules of different design, will be developed and presented in a full proposal anticipated for submission in mid-2015.

3.2.1 Dual Phase Option

The LBNO Collaboration is developing a dual-phase readout LAr-TPC in which the ionization electrons are drifted vertically in the liquid, extracted into the gas phase, and gas-amplified in a Large Electron Multiplier (LEM) stage before collection on the anode. The anode is assembled from modules that can be combined to produce a detector of any size[24, 25]. The LAr detector has the shape of a vertically standing cylinder, where electrons are drifted vertically towards the liquid-vapor interface (See Figure 15). The uniform drift field is created by an octagonal field cage composed of several equally-spaced stainless-steel tubes, supported by insulating mechanical structures which are suspended with stainless-steel ropes linked to the outer deck. The bottom field is closed by a transparent cathode and the top field by an anode, which also serves as the charge readout. Fully engineered and costed conceptual designs have been developed for the three mass options: 20, 50 and 100 kt, but optimized for the Pyhäsalmi mine location. All three configurations assume a 20 m long drift for the TPC, and are composed of modular charge and light readout located respectively at the top and bottom of the tank. The light readout consists of PMTs uniformly distributed below the cathode. A cost-optimized installation sequence for an underground location and associated logistics has been considered and developed. Work is presently ongoing to best implement the layout for a double-phase detector to the specificities of the SURF environment. In particular, the double-phase readout could be readily adapted to a different shape of the cryostat, such as the parallelepipedic membrane vessel embedded in the rock, proposed in the context of LBNE. With such a shape, a single unit double-phase detector with 23.3 kt active mass could be achieved with a

20m(w)x16m(drift)x52m(l) instrumented argon volume.

This new type of LAr-TPC, operating in the double-phase (liquid-vapor) mode in pure argon, is characterized by its charge amplifying stage (the LEM) and its projective anode charge readout system. Situated in the vapor phase on top of the active LAr volume, these provide an adjustable charge gain and two independent readout views, each with a canonical pitch of 3 mm. This pitch is optimal since the amplification stage produces sufficient charge to be shared among several readout electrodes operated in collection mode (smaller pitch sizes and more than two independent readout views could be considered), eliminating the drawbacks introduced by induction views. With t_0 time information provided by the LAr scintillation, they provide a real-time three-dimensional (3D) track imaging with dE/dx information and the detector acts as a high-resolution tracking-calorimeter. A high signal-to-noise ratio on 3 mm pitch or less, and a very low energy detection threshold (<100 keV) can be reached and maintained over very large active argon volumes in the LAr LEM-TPC thanks to the gas amplification stage, and therefore allows for long drift paths. The ionization charge is read out via cold-electronics embedded in the chimneys crossing the roof of the vessel. Although cold, because they are within the insulation layer of the cryostat, the front-end electronics remain accessible and upgradeable over the lifetime of the experiment without the necessity of emptying the main argon volume, removing the risk associated with failure of inaccessible active elements.

The performance of the double-phase readout has been extensively demonstrated with cosmic rays on small-scale devices up to 200 liters [26]. A test of a TPC with the scale of 1 m x 3 m anode plane and a 1-meter drift is currently under construction at CERN. It is planned to build a 6 m x 6 m x 6 m TPC demonstrator (WA105 approved experiment) [22] inside a 8 m x 8 m x 8 m cryostat, illuminated by a charged particle test beam, in the CERN Neutrino Platform. Construction has started for an extension of the EHN1 building in the North Area at CERN to house this and potentially the LBNE single-phase detector test, with the goal of executing initial beam tests before the start of the next long shutdown for LHC upgrades. The double-phase readout of the WA105 detector will be 36 m^2 or ≈1:30 of the required area for the 23.3 kt detector for SURF. Working as independent detector readout modules, scaling up from the 6x6x6 m^3 to the 23.3 kt will be straightforward and rely on the parallel production of 65 independent 4x4 m^2 readout units (see Figure 15 right), to be assembled and tested offsite before installation at SURF. The WA105 team also plans to develop and test a cathode high-voltage system up to 600 kV. All components such as cables, connectors, etc. used in the 400 kV industry standard are tested and must hold 600 kV. A 16 m drift considered for the 23.3 kt detector at SURF at a nominal drift field of 0.5 kV/cm and velocity of 1.5mm/μs would require an extrapolation to a cathode voltage of

800 kV. In the engineering design, a maximum field of 50 kV/cm for a conservative 2 MV has been imposed [25] therefore one expects a discharge free operation at the nominal drift field. For additional safety, one could also operate efficiently with a drift field of 0.4 kV/cm or ≈600 kV, reducing the electron drift velocity to 1.4mm/μs and taking advantage of the adjustable charge amplification in the LEM stage. The requirements on liquid argon purity for the double-phase design are similar to those for the single-phase design, since the large S/N ratio guarantees that 100% efficiency in hit reconstruction on both readout views, even after electron cloud diffusion over long paths, and potential charge attenuation due to attachment to the remaining traces of electronegative impurities.

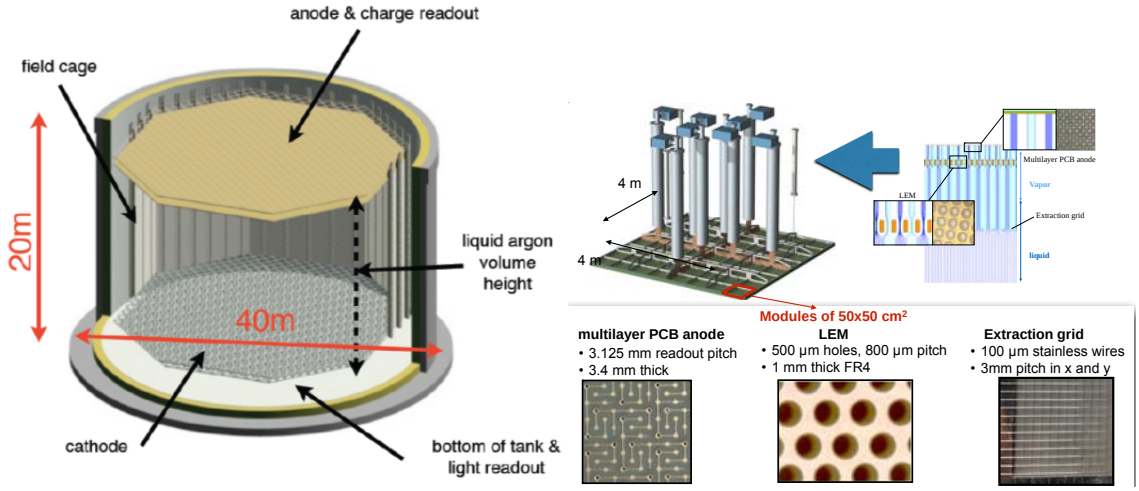

Figure 15. (left) Schematic view of the 20-kt double-phase LAr detector optimized for the Pyhäsalmi mine location. Engineering work is presently being performed to optimize the geometry to a SURF location (right) the basic 4x4 m² double-phase readout unit with their extraction, LEM amplifying stage and anode layer. In total 65 such units of 4x4 m² will be needed for the 23.3-kt detector.

3.2.2 Single Phase Option

The LBNE Collaboration is developing a design for a single-phase LAr-TPC in which the ionization electrons are drifted horizontally and collected directly in the liquid on wire planes without amplification[4, 27]. This design is based on the successful INFN ICARUS detector[28]. It takes a modular approach based on factory-built anode planes, which can be assembled in configurations and quantities depending on the total size of the far detector. Specific designs have been developed for 10 kt and 34 kt fiducial mass detectors.

The LAr TPC design (Fig. 16) utilizes a rectangular cryostat embedded directly in and supported by the rock in a dedicated cavern within SURF. This design

maximizes the use of the excavated volume and therefore maximizes the detector mass within cost constraints. The cryostat is divided into two identical modules to aid with detector commissioning (one cryostat can serve as a storage vessel for the other, if an early intervention is required) and to enhance uptime in case one detector must be off-line.

The TPC itself consists of alternating rows of cathode plane assemblies (CPAs) and anode plane assemblies (APAs). The modular design allows flexibility in the choice of anode-cathode spacing. Based on considerations of expected purity, signal-to-noise requirements and diffusion of the electron cloud, the spacing between CPA and APA rows has been set to 3.7 m. With an electric field of 500 V/cm, the maximum drift time is 2.3 ms. The single-wire detection threshold is estimated to be ≤1 MeV.

The APAs and CPAs are designed in a modular fashion and have dimensions 2.5m long and 7m high. See the right side of Fig. 16. Three sense wire planes (two induction planes and one collection plane) with wire pitches of 4.8 mm are mounted on each side of an APA frame, providing three views both for redundancy and to aid in reconstructing complex events. Wire pitch as low as about 3 mm has been considered, and the final configuration of wire pitch and stereo angle of the three views will be determined through both physics and cost optimization exercises currently in progress. During installation, two APAs are connected end-to-end to form a 14 m tall, 2.5 m long unit, and pairs of CPAs are installed in a similar fashion. This system of 2.5 m long detector elements is easily scalable to any desired detector size. A field cage for shaping the electric field covers the top, bottom, and ends of the detector. Scintillation light detectors, to provide the t_0 for the drift time measurement, consist of acrylic bars coated with wavelength shifter that are read out by silicon photomultipliers. These detectors are fitted within the gap between the wire planes on the two sides of the APA, thereby making efficient use of the space inside the cryostat.

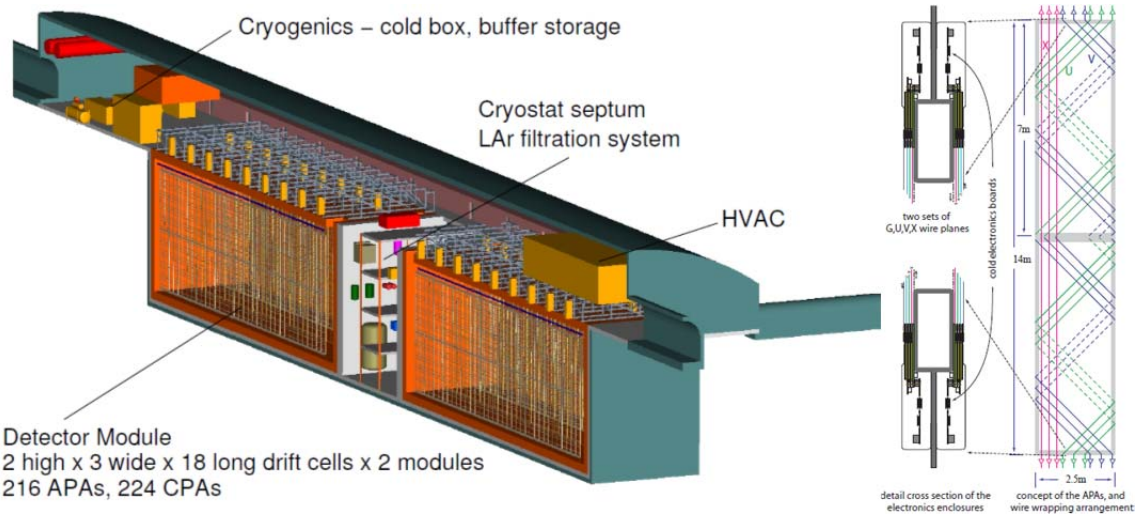

Figure 16. Schematic of a 34-kt fiducial mass LArTPC design (left) The detector comprises two 17-kt fiducial mass LArTPC detectors. The design of a pair of Anode Plane Assemblies is shown in the right-hand figure.

Low-noise, low-power CMOS preamplifier and ADC ASICS have been developed for deployment on circuit boards mounted directly on the APA frames. This scheme minimizes the capacitance to ensure good signal-to-noise performance. It offers the possibility of digital signal processing, including multiplexing and zero suppression at the front end, thereby limiting the cable plant within the cryostat and the number of penetrations required, while also easing requirements on the downstream readout and DAQ systems located outside the cryostat. The ASICS have been laid out following design rules developed explicitly for long-term operation at cryogenic temperatures. The same cold preamplifier is used in the MicroBooNE detector[29], which will allow an early and robust test of this design.

A complete cost estimate and resource-loaded schedule for the development, design, construction, installation and commissioning of the detector has been developed[30], and thoroughly reviewed by independent external review committees reporting to the Fermilab Director [31] and the U.S. Department of Energy[32].

The design of this detector is based on extensive R&D done as part of an integrated program of LAr TPC R&D, which includes: the Material Test Stand[33], which addresses issues related to argon purity; the Liquid Argon Purity Demonstrator[34], which has demonstrated the ability to achieve long electron lifetime in liquid argon without evacuation of the cryostat and now serves as a vessel for performing R&D tests of TPCs and other detector components; the ArgoNeuT detector[35], a small LAr TPC which was exposed to the NuMI beam;

and MicroBooNE[29], a 170 ton Liquid Argon Time Projection Chamber (LArTPC) which will begin taking data in the Fermilab Booster Neutrino Beam in early 2015.

A small-scale prototype, utilizing reduced-scale anode planes of the same conceptual design as those planned for the full detector, is currently being assembled inside a cryostat at Fermilab that can hold 35 tons of LAr. It will be tested with cosmic rays in the first half of 2015. An Expression of Interest [36] that contemplates a full-scale prototype for an engineering test in liquid argon and a beam test has been reviewed by the CERN SPSC and they have invited submission of a full technical proposal.

3.2.3 Other Development Programs

Other world-wide efforts on LAr TPC development which will also benefit the development of the LBNF far detector include the upgrades of the ICARUS detector (WA104)[37] for possible use in a short-baseline program at Fermilab, MicroBooNE[29], the proposed LAr1-ND experiment[38] at Fermilab, the LArIAT test beam program[39], ARGONCUBE[40], and other smaller scale R&D programs.

3.3 Fine Grained Near Detector

The LBNF Near Detector is required to:

- Measure the relative abundance and energy spectrum of all four species of neutrinos in the LBNF beam, muon-neutrino (ν_μ), muon-antineutrino ($\overline{\nu}_\mu$), electron-neutrino (ν_e), and electron-antineutrino($\overline{\nu}_e$), to a few percent;
- Determine the absolute neutrino and antineutrino flux to measure the cross sections to ~3%, precision necessary to interpret the far detector signal and backgrounds;
- Quantify the asymmetries between neutrinos and anti-neutrinos, including energy scales and interaction topologies, for the CP-violating phase;
- Predict the Far Detector flux relative to Near Detector, FD/ND, to within a few percent for all four species;
- Measure the backgrounds to the oscillation signal, i.e. π^0, π^-, and π^+ yields, both in charged-current (CC) and neutral-current (NC) interactions;
- Characterize various exclusive (semi-exclusive) channels such as Quasi-Elastic (QE), Resonance (Res), Coherent-mesons and Deep-Inelastic-Scattering (DIS);
- Quantify the neutrino-nucleus cross-sections by measuring interactions off nuclear targets, most notably Ar and Ca targets, to account for nuclear

effects while interpreting the FD signal; and

- Provide rich physics, comprising a generational advance in the precision measurements and sensitive searches unique to neutrinos.

To meet the above requirements, a high resolution, magnetized near detector capable of measuring negative & positive muons and electrons with high efficiency is needed. The reference design of the Near Detector is a fine-grained tracker (FGT, see Fig. 17), which consists of a large-volume straw-tube tracking detector and electromagnetic calorimeter inside of a dipole magnet, and resistive plate chambers for muon identification located in the magnet yoke and upstream and downstream steel absorbers[14]. High-pressure argon gas targets and other nuclear targets are embedded in the upstream part of the tracking volume. This design may be augmented by a LAr or GAr TPC to improve calibration of reconstruction efficiencies in the far detector.

This detector is required to be of low-density with a commensurately long physical radiation length for the footprint of an event's constituent particles to be sufficiently distinct. The near detector would include (1) high fidelity identifications of μ^-, μ^+, e^- and e^+ to ID the four neutrino species, the e^-/e^+ ID also being necessary to measure the photons to reconstruct the π^0; (2) good momentum and dE/dx resolution to measure the charged hadrons (π^+, π^-, p, K^+, K^-) (see Fig. 18), and neutral hadrons (π^0, K^0, Λ); (3) adequate containment to reconstruct the 3-momenta of the particles; (4) fast-readout to handle the event rates; (5) nuclear targets, including Ar & Ca, to measure empirically not only the ν-Ar effects but to precisely model these effects (see Fig. 19); (6) sufficient target mass to provide an order of magnitude higher systematic and statistical precision than in the current most precise experiment; (7) 4π calorimetric and muon coverage to measure neutral hadrons and muons, and to veto particles from outside. Requirement (5) is that one of the target nuclei is the same as that in the far detector to allow cancellation of some systematic errors; the inclusion of other target nuclei would provide constraints for accurate modeling of nuclear effects.

Such a detector, placed in the high-intensity neutrino beam needed for the oscillation measurements, will collect a vast sample of neutrino interactions. This will enable a rich program in neutrino scattering physics addressing many non-oscillation topics, such as neutrino cross sections, precision electroweak measurements, and searches for new physics.

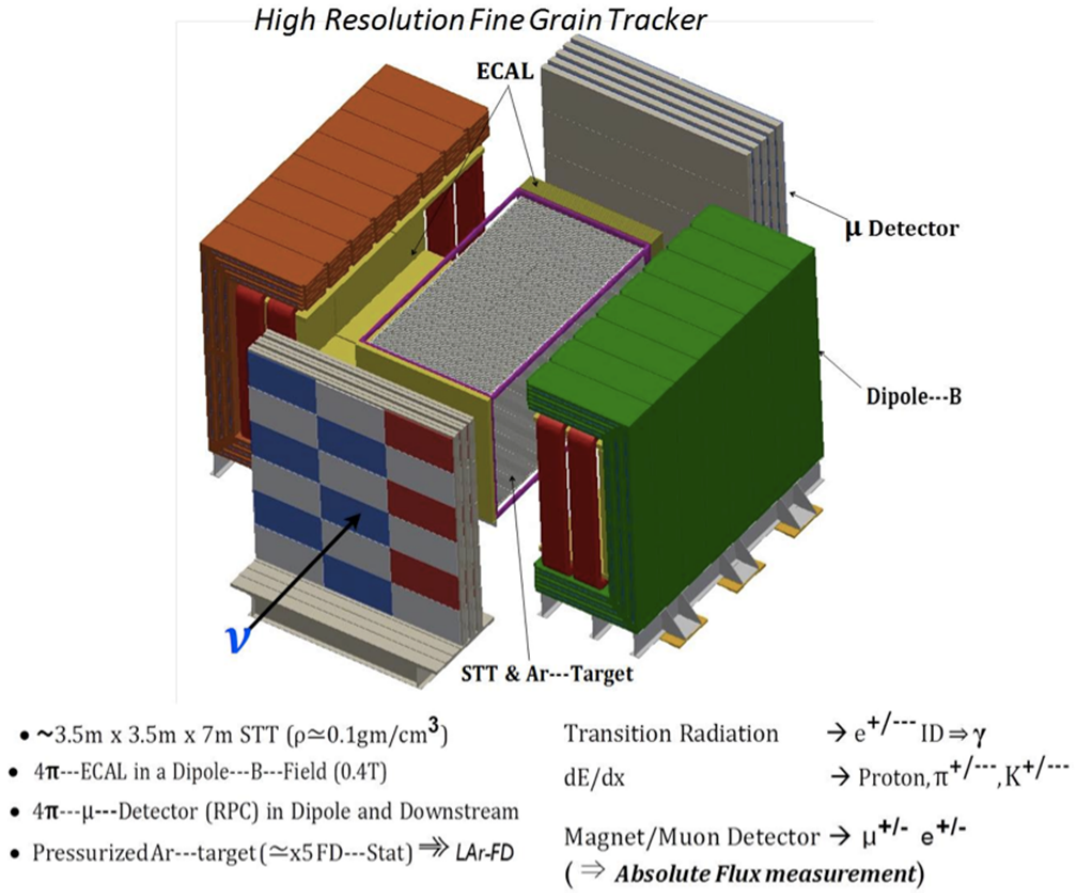

Figure 17: Schematic of the Fine-Grained Tracker Near Detector, with straw-tube tracker (STT), electromagnetic calorimeter (ECAL), large-aperture dipole magnet, and resistive plate chamber (RPC) muon detectors.

The active target is composed of the straw tube tracker (STT) equipped with the transition radiation (TR) capability to distinguish electron/positron (with Lorentz factor >1000) from muon/pions with high efficiency and purity. The low average density of the target, ~0.1 g/cm^3 (similar to that of liquid hydrogen), combined with the granularity of the STT, provides excellent momentum and angular resolutions for μ^+, μ^-, e^+, e^-, π^+ ,π^-, π^0, proton, and K^0 produced in ν-induced interactions – see Figure 18.

The proposed FGT would fulfill the near detector requirements introduced above. In particular, the near detector would: (1) characterize the neutrino source extremely well including a measurement on ν_e/ν_μ and $\overline{\nu}_e/\overline{\nu}_\mu$ with 1% precision or better; (2) measure the absolute neutrino flux using neutrino-electron scattering with 3% precision or better; (3) determine the energy scale and topologies of neutrino and antineutrino interactions; (4) accurately classify NC and CC interactions and determine the yields of $\pi^0/\pi^-/\pi^+$ dominant backgrounds to the oscillation signal from each; (5) measure the (semi-)exclusive processes such as

QE, Resonance, Coherent-Meson; and (6) conduct a rich panoply of measurements and searches unique to the neutrino physics engendering over 120 topics which over the lifetime of the experiment would lead to more than two hundred papers and Ph.D. theses.

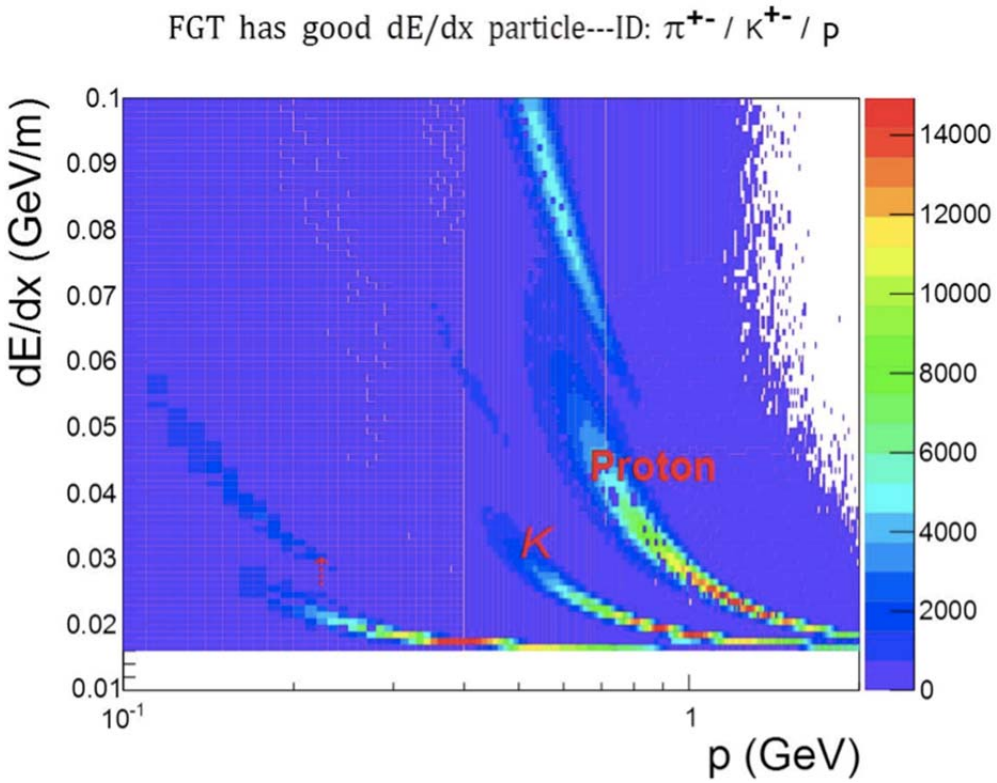

Figure 18: Simulation of dE/dx versus momentum measured in the straw-tube tracker for hadrons produced in charged-current interactions.

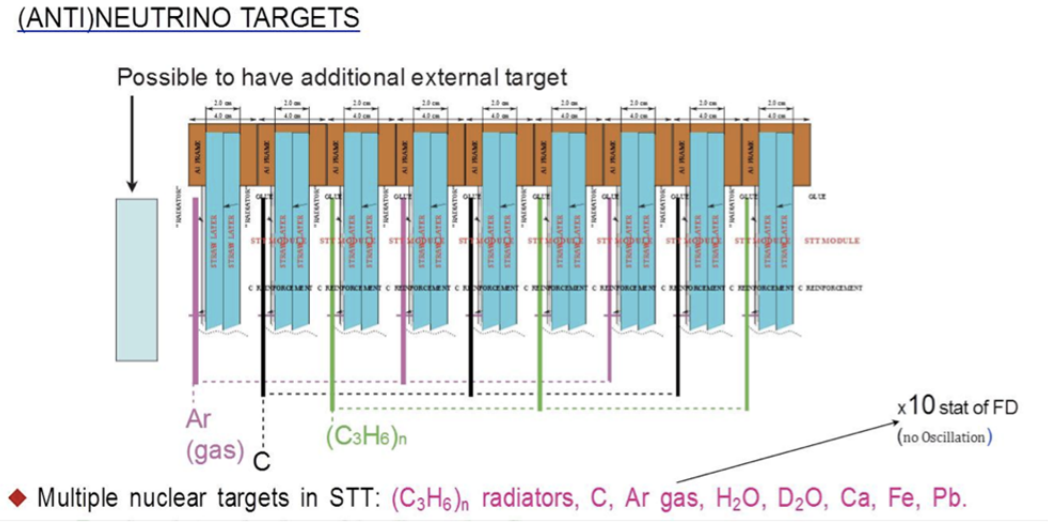

Figure 19: Schematic of nuclear targets (Ar, Ca, C, etc.) placed at the upstream end of the FGT. Note that pressurized Ar gas will be placed in aluminum tubes.

Of note for this near detector concept is that since the FGT is not identical to the far detector it is not possible in long-baseline analyses to 'cancel' the event reconstruction errors in a near to far ratio, done for example in MINOS. The extent to which such a cancellation will limit the ultimate precision of the experiment has yet to be fully explored. However, at the international Near Neutrino Detector workshop held at Fermilab (July 2014)[41] it was accepted that the FGT offers a sound basis for moving forward but also that a LAr TPC or high-pressure gaseous-argon TPC placed upstream of the FGT would enhance the near detector capability.

Conceptual designs for a standalone magnetized LAr TPC near detector[42] and a standalone gaseous argon TPC near detector[43] have been developed and could serve as starting points for the design of this addition to the FGT. Significant simulation and engineering study is required to understand whether a liquid or gas argon TPC is best for minimizing systematic errors in the long-baseline measurements and to integrate the additional detector system with the FGT design to make a coherent near detector system.

3.4 The Neutrino Beamline

The Beamline is a central component of LBNF and takes as its driving physics considerations the long-baseline neutrino oscillation analyses. The design as of the end of 2012 is fully described in [10]. Design work has continued since then both to develop the engineering design and to improve the capability of the beam for long-baseline physics. The significant design improvements include: increasing the initial beam power handling capability of all components to 1.2 MW, demonstrating that the focusing horns can be operated at 230 kA, and changing the decay pipe design from air-filled to helium-filled. This section briefly sketches the current design. Additional possible improvements have been discussed in Section 2.1.3. CERN has also developed a design for a long-baseline beamline optimized for 2300 km as part of the LAGUNA-LBNO Design Study [11] and initial discussions have begun to incorporate ideas from this design into the LBNF beamline design.

The LBNF beamline will aim a beam of neutrinos from Fermilab, with a 5.8° downward vertical bend, toward detectors placed at the Sanford Underground Research Facility (SURF) in South Dakota, about 1,300 km away. It is a wide-band (broad energy range), sign-selected beam, aiming to cover both the first and second oscillation maxima. The initial beam power is expected to be ~1.2 MW, however the facility is designed to be upgradeable for 2.4 MW operation. The Beamline design has benefited significantly from the design and operational experience of the NuMI beamline which is in operation since 2005.

The Beamline facility is expected to be fully contained within Fermilab property and its main elements are a primary proton beamline, a neutrino beamline, and conventional facilities to support the technical components of the proton and neutrino beamlines. The primary proton beam, in the energy range of 60-120 GeV, will be extracted from the Main Injector's (MI) MI-10 straight section using "single-turn" extraction. The beam is then transported with negligible losses to the target area within a beam enclosure embedded in an earthen, engineered filled embankment (hill) whose dimensions are commensurate with the bending strength of the required dipole magnets (see Figure 20). For 120 GeV operation and with the MI upgrades implemented for the NOvA experiment as well as with the expected implementation of the accelerator Proton Improvement Plan, phase II (PIP-II), the fast, single turn extraction will deliver all the protons (7.5×10^{13}) in one MI machine cycle (1.2 sec) to the LBNE target in 10 μs. The accelerator complex and the primary beamline are planned to deliver about 11×10^{20} primary protons to the neutrino target per year for 1.2 MW operation for an uptime of 56%.

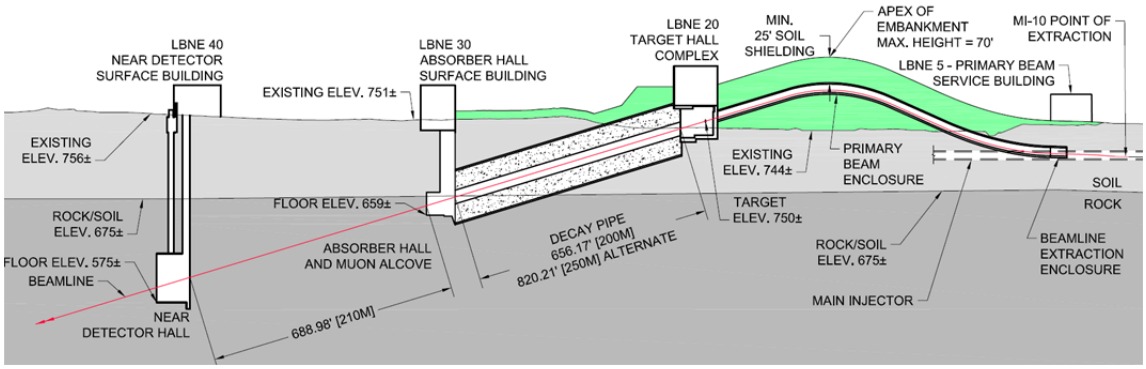

Figure 20: Longitudinal section of the LBNF beamline facility at Fermilab. The beam comes from the right, the protons being extracted from the MI-20 straight section of the Main Injector.

Neutrinos are produced after protons from the Main Injector hit a solid target where approximately 85% of the protons interact producing pions and kaons which are subsequently focused by two magnetic horns into a decay pipe where they decay into muons and neutrinos. The neutrinos form a wide-band, sign-selected neutrino or anti-neutrino beam, designed to provide flux in the energy range of 0.5 to 5 GeV.

The reference target design for LBNF is an upgraded version of the NuMI-LE (Low Energy) target design that was used for 7 years to deliver beam to the MINOS experiment and was exposed to beam power up to 375 kW. The target is made out of graphite, it is segmented and about one meter long, and it is mounted together

with a baffle on a carrier allowing for the flexibility to move the target with respect to the focusing devices, and therefore for a tunable neutrino energy spectrum. Focusing of charged particles is achieved by two magnetic horns in series, the first of which partially surrounds the target (see Fig. 21). They are both NuMI/NOvA design horns with double paraboloid inner conductor profiles and currents of up to 230 kA.

The decay volume in the LBNF reference design is a helium-filled, air-cooled pipe of circular cross section with its diameter (4 m) and length (204 m-250 m) optimized such that decays of the pions and kaons result in neutrinos in the energy range useful for the experiment. A 250-m decay pipe is the maximum length that will allow the near neutrino detector complex to fit within the Fermilab site boundaries. At the end of the decay region, the absorber, a water-cooled pile of aluminum and steel, is needed to remove the residual particles remaining at the end of the decay pipe. An array of muon detectors located in a small muon alcove immediately downstream of the absorber provide information on the direction, profile and flux of the neutrino beam.

In general, components of the LBNE beamline system that cannot be replaced or easily modified after substantial irradiation during 1.2 MW operation are being designed to for operation at 2.4 MW. Examples of such components are the shielding of the target chase and decay pipe, the absorber with its associated shielding and the remote handling.

In order to increase the neutrino event rates and before baselining the experiment we are considering:

- Development of more optimized horn designs which could boost the flux, especially in the low-energy region below the peak of the first oscillation maximum and down to the second oscillation maximum.
- Using materials for the target alternate to graphite (e.g. Be) to increase the target longevity, as well as investigating different target shapes and dimensions. This would involve additional R&D effort.
- Increasing the length of the decay pipe up to 250 m (the maximum length allowed by the existing Fermilab site boundaries), and possibly the diameter of the decay pipe up to 6 m.

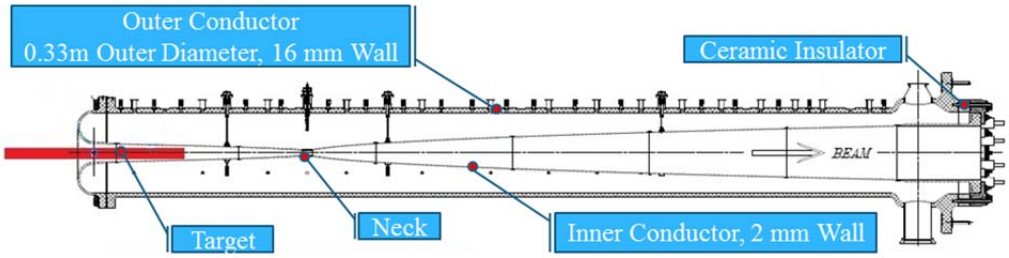

Figure 21: Longitudinal section of the first focusing horn with the target inserted into it. A current of 230 kA through the inner and outer conductors generates a toroidal field between the conductors (~3.4 T at the neck). A second horn, 6.6 m downstream, provides additional focusing to secondary particles.

3.5 Sanford Underground Research Facility

The Sanford Underground Research Facility (SURF) in Lead, South Dakota, a dedicated deep underground research facility, has been selected as the location of the far detector for the proposed Figure 22 illustrates Sanford Laboratory's location within the region as a part of the northern Black Hills of South Dakota.

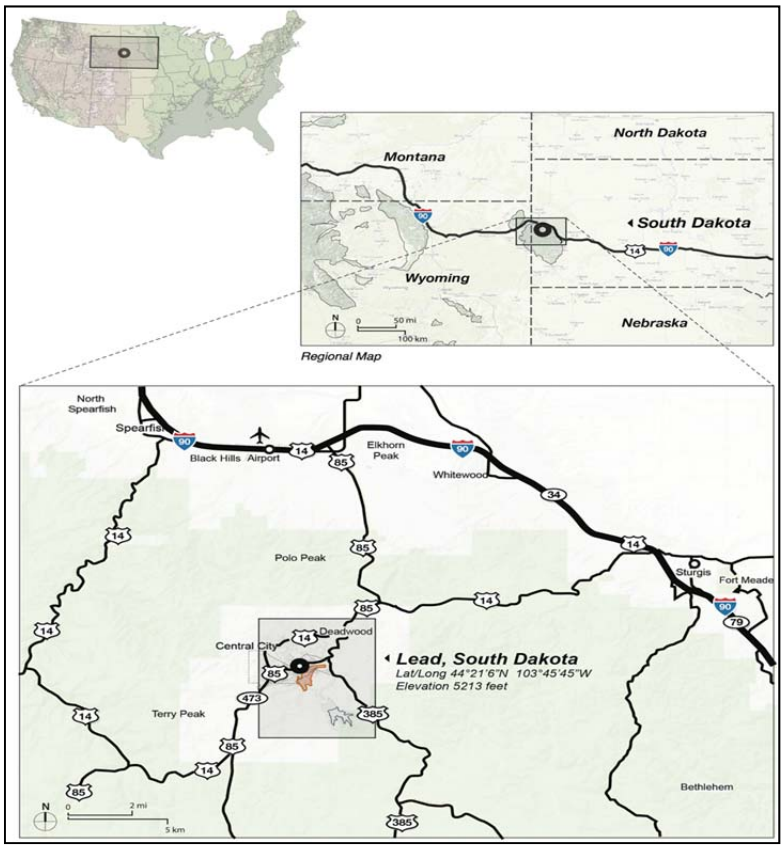

Figure 22. SURF's Regional context showing the city of Lead, South Dakota.

SURF is being developed in the former Homestake Gold Mine. Barrick Gold Corporation donated the site to the State of South Dakota in 2003, following over 125 years of mining. Mining operations created over 600 km of tunnels and shafts in the facility, extending from the surface to over 8000 feet below ground. The mining levels are distributed ~150 feet apart and are referenced by the feet below the entrance to the facility, therefore the level 4850 feet below ground is referred to as the 4850L. A historic cross section of the Homestake Mine is presented in Fig. 23.

The South Dakota Science and Technology Authority (SDSTA) operates and maintains the Sanford Laboratory at the Homestake site in Lead, South Dakota through a contract managed and overseen by Lawrence Berkeley National Laboratory's (LBNL)'s SURF Operations Office. The Sanford Laboratory property comprises 186 acres on the surface and 7,700 acres underground. The Sanford Laboratory Surface Campus includes approximately 253,000 gross square feet of existing structures. Using a combination of private funds, South Dakota Legislature-appropriated funding, a US Federal HUD Grant, and funding from NSF and DOE, the SDSTA has made significant progress in stabilizing and rehabilitating the Sanford Laboratory facility to provide for safe access and prepare the site for science experiments. The DOE now supports the operation of the facility, in addition to state and private funding. Both the NSF and the DOE support experiments at the site.

The science program at SURF for roughly the next five years is concentrated at two campuses located near the two main access shafts at the 4850L, the Davis Campus – site of the former Homestake Neutrino Experiment, and the Ross Campus as shown in Figure 24. The near term scientific program at SURF consists of the MAJORANA DEMONSTRATOR (MJD) neutrinoless double beta decay experiment, the Large Underground Xenon (LUX) dark matter search, the Center for Ultralow Background Experiments at Dakota (CUBED), and geoscience installations. Plans are being developed to host the Far Detector proposed here, a nuclear astrophysics program involving underground particle accelerators (CASPAR), and second and third generation dark matter experiments. Additional details concerning SURF can be obtained from the Homestake DUSEL Preliminary Design Report[44].

The LAr far detector will be located in new excavated spaces near the bottom of the Ross Shaft, about 1 km from the Davis Campus as shown in Figure 24. The 4,850-ft depth (4300 mwe) makes it an extremely competitive location in terms of cosmic-ray background suppression for undertaking the nucleon decay and supernova neutrino studies that this experiment plans to address. Another advantage of the proposed 4850L location for the far detectors is the low level of rock radioactivity

that could contribute backgrounds to the supernova burst neutrino signal and other low-energy physics searches. It was found that the U/Th/K radioactivity for the underground bedrocks at SURF is in general very low when compared to common construction materials such as concrete and shotcrete[4].

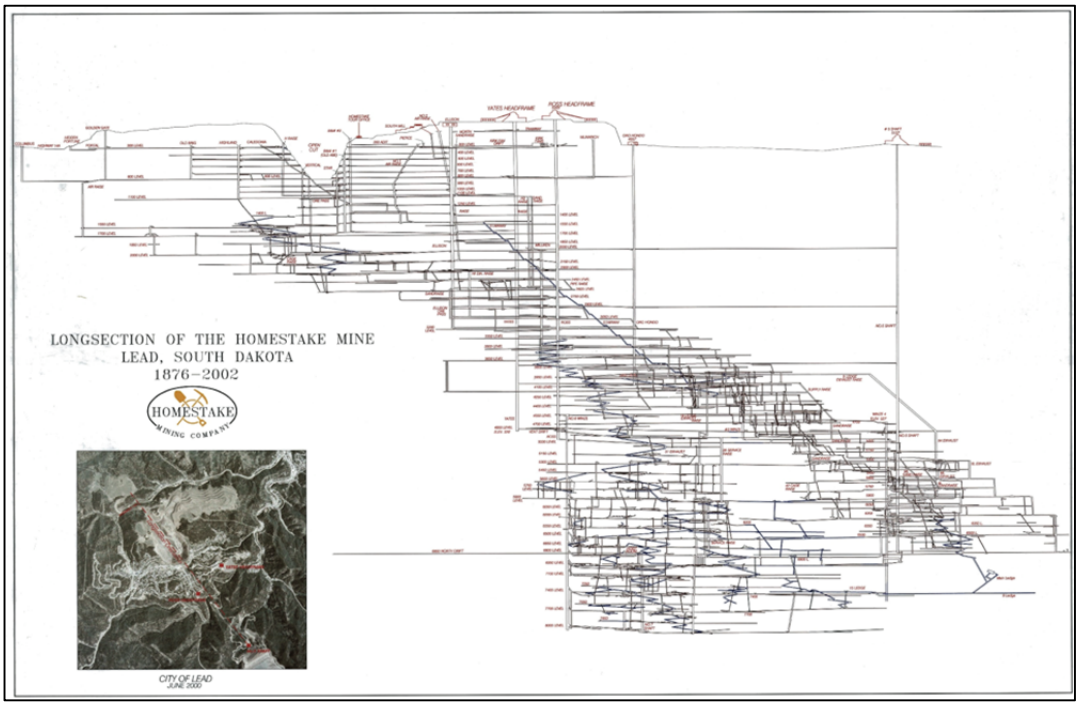

Figure 23. The long section of the former Homestake Gold Mine. This figure illustrates the 60 underground levels extending to greater than 8,000 feet below ground. The location of cross section is indicated in the inset along a NW to SE plane. The projection extends for 5.2 km along this plane.

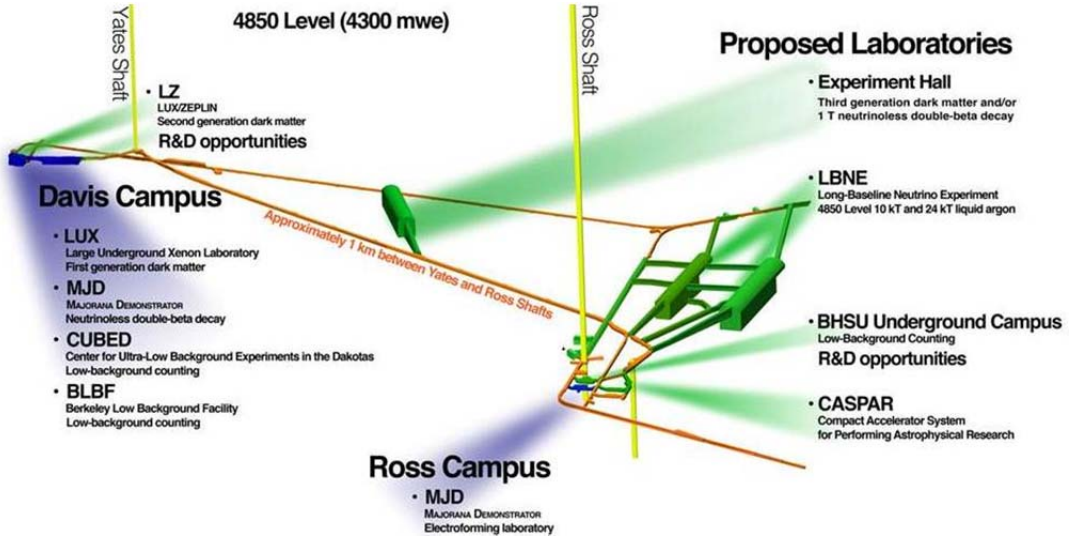

Figure 24. The 4850 (4300 mwe) level of SURF highlighting the existing and proposed experiments.

4.0 Organization: The Experiment and The Facility

It is envisioned that the experimental program proposed in this LOI and the LBNF facility would be two distinct entities. The international partners may contribute to either or both.

The experimental program collaboration will be responsible for:

- The definition of the scientific goals and corresponding scientific and technical requirements on the detector systems and neutrino beam line.
- The design, construction, commissioning and operation of the detector systems.
- The scientific research program conducted with the detectors and LBNF neutrino beam.

Fermilab will provide the high-intensity proton source that will drive the long-baseline neutrino beam, utilizing the existing Main Injector with upgraded injectors (PIP-II)[9]. PIP-II is also being planned with significant international collaboration. Fermilab, working with and with the support of international partners, will be responsible for the Long-Baseline Neutrino Facility, including:

- Design, construction and operation of the LBNF beamline, including the primary proton beam beamline and the neutrino beamline including target, focusing structure (horns), decay pipe, absorber, and corresponding beam instrumentation.
- Design, construction and operation of the conventional facilities and technical infrastructure on the Fermilab site required for the Near Detector complex.
- Design, construction and operation of the conventional facilities and technical infrastructure within the Sanford site, including cryostat and cryogenic systems, required for the Far Detector.
- Fermilab, as the host lab, will pay for the operating costs of the facility.

Close and continuous coordination between the collaboration and LBNF will be required to ensure the success of the combined enterprise. An Experiment-Facility Interface Group will be established (by Fermilab) to oversee and ensure the required coordination both during the design and construction and the operational phases of the facility and the experiment. This Group will cover areas including

- Interface between the Near and Far Detectors and the corresponding conventional facilities.
- Interface between the detector systems provided by the collaboration and the technical infrastructure provided by LBNF.

- Design and operation of the LBNF neutrino beamline. This is a particularly important activity, since the neutrino-energy spectrum and other characteristics of the neutrino beam, and the ability to measure those characteristics, are a crucial part of the long-baseline experimental program.

The successful model used by CERN for managing the construction and exploitation of the LHC and its experiments will be used as a starting point for the joint management of LBNF and the experimental program. Fermilab, as the host laboratory, will have responsibility for the facilities, and for oversight of the experiment and its operations. Mechanisms to ensure input from and coordination among all of the funding agencies supporting collaboration, modeled on the CERN Resource Review Board, will be adopted. The same (or similar) structure will be employed to coordinate among funding agencies supporting the LBNF construction and operation.

5.0 Scientific and Experimental Strategy

Achieving the conditions described in the previous sections is necessary for the previously independent worldwide experimental options to converge on a single facility and for the creation of a unique international collaboration with the capabilities to develop a world-class experiment with FNAL acting as host. The new collaboration supporting this LOI includes key international players in ongoing supporting programs (such as the CERN Neutrino Platform) and is in the unique position to propose a credible and effective experimental plan supported by a "Conceptual Design Report" (CDR) to be submitted in the summer of 2015. A fully established cost and schedule (CD-2) will follow by the end of 2017.

We propose a strong and timely strategy to benefit from the unique opportunity provided by LBNF:

- This collaboration will rapidly establish a world-class program in the deep underground physics (accelerator and non- accelerator) through the construction of a modular set of detectors that are not necessarily identical but are of the similar mass.

- The construction of an initial 10-kt detector deep underground at Sanford laboratory on a timescale of 2021 is a top priority to begin the physics program and establish the collaboration in the neutrino landscape. This early first module installation will engage the collaboration, test all the aspects of

the underground installation and operation, and will provide an early underground physics program as well as be ready for beam physics as soon as PIP-II is implemented.

- Remaining modules will follow in rapid succession in order to complete the 40 kt detector in a timely fashion.

- The new international collaboration will leverage the CERN Neutrino Platform as an important facility for detector design and development. The collaboration will also utilize the infrastructure of both its university partners and science laboratories located around the world.

- The collaboration will have the necessary expertise, intellectual resources and critical mass to accrete the financial resources to design and implement this challenging plan.

- We expect to start data taking from accelerator operations in 2024 and extend until around 2035 (a decade of beam operations) in order to fully exploit this remarkable facility.

- Our experiment offers a unique, exciting and challenging program that adopts a modular approach to get first science early and drive the establishment of the facility that will lead to the scientific discoveries that are core to the LBNF program.

6.0 Plan for Development of the Conceptual Design Report

6.1 Key Strategic Questions

There are a number of key strategic decisions that will need to be addressed by the collaboration as part of the writing of the CDR. For illustration, a sample of the issues to be addressed include:

- Examine the tradeoffs between a single large cavern as compared to multiple smaller, modular caverns.

- Determine the optimal construction strategy. Is it better to clone identical modules or to construct detectors with increasing volumes (as risks are mitigated)?

- Based on a given funding profile, how should the funds be allocated to optimize the scientific impact. When does a finely segmented near detector need to be in place?

- When does the neutrino beam line need to be completed – when PIP-II is ready or earlier in order to exploit 700 kW beam currently serving NOvA?

- Define the final mix of technologies. Should the LAr technology be single phase, two-phase, or a combination of both?

- Consider the benefits of constructing a small (approximately 100 ton) demonstrator before 2021 in the underground laboratory at Sanford in order to retire technical/implementation risks.

- Determine the timeline for key decisions and establish milestones, such as CD-2/3 reviews to drive the program forward.

- Determine the roadmap to produce "CD-1 like" documentation (with detailed costing) within the coming year.

6.2 Immediate Plan

Due to the scientific importance of the proposed experimental program and the urgency to take advantage of the positive developments in support of LBNF, the intention is to form the full collaboration structure on a rapid timescale. In particular, as soon as possible, we as the newly forming collaboration intend to:

- Establish the collaboration, implement a governance model, and choose leadership for the collaboration.
- Determine the roadmap for the completion of the writing of a CDR and for the provision of the "CD-1 like" supporting material including a cost and schedule within the coming year.

7.0 Summary and Conclusions

This LOI expresses the intent of a new international collaboration to perform a world-leading experimental program in neutrino oscillations, neutrino scattering physics, nucleon decay searches, and neutrino astrophysics. It proposes to utilize the planned Long-Baseline Neutrino Facility to build a large state-of-the-art liquid argon detector deep underground in the Sanford Underground Research Facility and a high-precision near neutrino detector on the Fermilab site. The experiment

will exploit the planned high-intensity LBNF neutrino beam driven by a 1.2 MW proton beam enabled by the PIP-II accelerator upgrade at Fermilab, which can be upgraded to provide 2.4 MW in the future. It will also exploit the expanded underground access enabled by renovations of SURF and the excavation of large caverns for this experiment. The far detector is planned to have a fiducial mass of approximately 40 kt operational by the middle of the next decade. An important intermediate milestone is to deploy an initial 10-kt underground detector on the timescale of 2021. Beam operations with the full scope detector would begin several years after that and continue for more than a decade.

The new collaboration has combined expertise in long-baseline oscillations, underground physics and neutrino scattering physics, as well as extensive experience in the detector technologies critical for this experiment. The experiment plan is based on more than a decade of detailed design studies and detector development by many groups that are now joining together to form the new collaboration. The collaboration plans to develop this LOI into a full technical proposal as rapidly as possible. The immediate goal is to complete the experiment design, documented in a full Conceptual Design report and corresponding project plan, within the coming year and to move rapidly to start building the experiment.

References

[1] H. Nunokawa, S. J. Parke, and J. W. Valle, Prog.Part.Nucl.Phys. **60**, 338 (2008), 0710.0554.

[2] P. Huber *et al.*, Comput. Phys. Commun. **167**, 195 (2005).

[3] P. Huber *et al.*, 2007, arXiv:hep-ph/0701187.

[4] LBNE Collaboration, C. Adams *et al.*, The Long-Baseline Neutrino Experiment: Exploring Fundamental Symmetries of the Universe, 2014, 1307.7335.

[5] M. Gonzalez-Garcia, M. Maltoni, and T. Schwetz, JHEP **1411**, 052 (2014), arxiv 1409.5439.

[6] LAGUNA-LBNO Collaboration, S. Agarwalla *et al.*, JHEP **1405**, 094 (2014), 1312.6520.

[7] X. Qian *et al.*, Phys.Rev. **D86**, 113011 (2012), 1210.3651.

[8] M. Blennow, P. Coloma, P. Huber, and T. Schwetz, (2013), 1311.1822.

[9] P. Derwent et al., Proton Improvement Plan-II (2103), Project X-doc-1232, http://projectx-docdb.fnal.gov/cgi-bin/RetrieveFile?docid=1232&filename=1.2%20MW%20Report_Rev5.pdf&version=3

[10] LBNE Project, Conceptual Design Report Volume 2: The Beamline at the Near Site, LBNE-doc-4317 (2012), http://lbne2-docdb.fnal.gov/cgi-bin/

RetrieveFile?docid=4317&filename=CDR-beam-volume-101812-reduced.pdf&version=25

[11] The LAGUNA-LBNO Consortium, Conceptual Design of a Conventional Neutrino Beam from CERN to Pyhäsalmi, (2014), http://laguna.ethz.ch:8080/Plone/deliverables/laguna-lbno-284518-deliverables/conceptual-design-of-a-conventional-neutrino-beam-from-cern-to-pyhasalmi/at_download/file

[12] MINOS Collaboration, P. Adamson *et al.*, Phys.Rev.Lett. **110**, 171801 (2013), 1301.4581.

[13] T2K Collaboration, K. Abe *et al.*, Phys.Rev.Lett. **112**, 061802 (2014), 1311.4750.

[14] B. Choudhary et al., Proposal of Indian Institutions and Fermilab Collaboration for Participation in the Long-Baseline Neutrino Experiment at Fermilab, LBNE-doc-6704(2012), http://lbne2-docdb.fnal.gov/cgi-bin/RetrieveFile?docid=6704&filename=LBNE-India-DPR-V12-Science_smaller.pdf&version=1

[15] D. Angus *et al.* [LAGUNA Collaboration], arXiv:1001.0077 [physics.ins-det].

[16] A. Bueno, Z. Dai, Y. Ge, M. Laffranchi, A. J. Melgarejo, A. Meregaglia, S. Navas and A. Rubbia, JHEP **0704**, 041 (2007) [hep-ph/0701101].

[17] K. Scholberg, Ann. Rev. Nucl. Part. Sci. **62**, 81 (2012) [arXiv:1205.6003 [astro-ph.IM]].

[18] H. Minakata, H. Nunokawa, R. Tomas and J. W. F. Valle, JCAP **0812**, 006 (2008) [arXiv:0802.1489 [hep-ph]].

[19] L. Hudepohl, B. Muller, H.-T. Janka, A. Marek and G. G. Raffelt, Phys. Rev. Lett. **104**, 251101 (2010) [Erratum-ibid. **105**, 249901 (2010)] [arXiv:0912.0260 [astro-ph.SR]].

[20] K. Scholberg *et al.*, "SNOwGLoBES: SuperNova Observatories with GLoBES." {http://www.phy.duke.edu/~schol/snowglobes}.

[21] http://iifc.fnal.gov/

[22] C. Rubbia, The liquid-Argon time projection chamber: a new concept for neutrino detector, CERN-EP-77-08 (1977)

[23] I. De Bonis et al. (The LBNO-DEMO (WA105) Collaboration), Technical Design Report for large-scale neutrino detectors prototyping and phased performance assessment in view of a long-baseline oscillation experiment, CERN-SPSC-TDR-004, arXiv:1409.4405 (2014) and references therein.

[24] A. Stahl et al., Expression of Interest for a very long baseline neutrino oscillation experiment (LBNO), CERN-SPSC-2012-021 (2012)

[25] The LAGUNA-LBNO Consortium, LAGUNA-LBNO DESIGN STUDY (2014) http://laguna.ethz.ch:8080/Plone/deliverables/laguna-lbno-284518-deliverables

[26] A. Badertscher et al., NIM A641, 48-57 (2011); Ibid, NIM A 617, 188 (2010); Ibid, JINST 7 (2012) P08026; Ibid, JINST 8 P04012 (2013); C.Cantini et al., JINST 9, P03017 (2014); Ibid, arXiv:1412.4402.

[27] The LBNE Project, Conceptual Design Report Volume 4: The Liquid Argon Detector at the Far Site, LBNE-doc-4892-v8 (2012), http://lbne2-docdb.fnal.gov/cgi-bin/RetrieveFile?docid=4892&filename=volume-4-LAr-rev1.pdf&version=8; B. Norris et al., LBNE Conceptual Design Document of the Cryogenic System that serves the LAr-FD 34 kton detector at 4850', LBNE-doc-7523 (2103), http://lbne2-docdb.fnal.gov/cgi-bin/RetrieveFile?docid=7523&filename=Cryo%20System%204850%20for%2034%20kton%20fiducial%20mass%20July%2023%202013.pdf
[28] C. Rubbia et al., JINST 6 P07011 (2011) and references therein.
[29] http://www-microboone.fnal.gov/index.html
[30] http://lbne.fnal.gov/reviews/CD1-review-top.shtml#Cost, see section "LBNE Cost and Schedule Documents"
[31] Final Report Director's Independent Conceptual Design and CD-1 Readiness Review of the LBNE Project, March 2012, http://www.fnal.gov/directorate/OPMO/Projects/LBNE/DirRev/2012/03_26/FinalReportDirector%27sReviewLBNE2012-03-30.pdf
[32] Department of Energy Review Committee Report on the Technical, Cost, Schedule, and Management Review of the Long Baseline Neutrino Experiment (LBNE), October 2012, http://www.fnal.gov/directorate/OPMO/Projects/LBNE/DOERev/2012/10_30/1210_LBNE_rpt.pdf
[33] B. Rebel et al., J.Phys.Conf.Ser. 308 (2011) 012023.
[34] M. Stancari et al., The Liquid Argon Purity Demonstrator, LARTPC-doc- 1176 (2014), http://lartpc-docdb.fnal.gov/cgi-bin/RetrieveFile?docid=1176&filename=LAPD.pdf&version=1
[35] C. Anderson et al., The ArgoNeuT Detector in the NuMI Low-Energy Beam Line at Fermilab, JINST 7 P10019 (2012).
[36] M.A.Leigui de Oliveira, Expression of Interest for a Full-Scale Detector Engineering Test and Test Beam Calibration of a Single-Phase LAr TPC, CERN-SPSC-2014-027 (2014)
[37] C. Montanari et al. (ICARUS Collaboration). ICARUS: The project WA104 at CERN and P-1052 at Fermilab, http://indico.cern.ch/event/309151/session/0/contribution/0/material/slides/
[38] C. Adams et al., LAr1-ND: Testing Neutrino Anomalies with Multiple LAr TPC Detectors at Fermilab, Fermilab proposal P-1053 (2013), http://www.fnal.gov/directorate/program_planning/Jan2014PACPublic/LAr1ND_Proposal.pdf
[39] http://intensityfrontier.fnal.gov/lariat.html
[40] Igor Kreslo, Modular scalable TPC for neutrino observatories, indico.cern.ch/event/345706/session/0/contribution/0/material/slides/0.pdf (2014)
[41] https://indico.fnal.gov/conferenceDisplay.py?confId=8125

[42] The LBNE Project, Conceptual Design Report Volume 3: Detectors at the Near Site, LBNE-doc-4724-v10 (2012), http://lbne2-docdb.fnal.gov/cgi-bin/RetrieveFile?docid=4724&filename=volume-3-ND.pdf&version=10

[43] The LAGUNA-LBNO Consortium, Conceptual Design of a Conventional Neutrino Beam from CERN to Pyhäsalmi, Chapter 8, pp. 335-355, (2014), http://laguna.ethz.ch:8080/Plone/deliverables/laguna-lbno-284518-deliverables/conceptual-design-of-a-conventional-neutrino-beam-from-cern-to-pyhasalmi/at_download/file]

[44] Lesko, K.T., et al., "Deep Underground Science and Engineering Laboratory - Preliminary Design Report", arXiv:1108.0959, (2012)

Appendix A – Signatures

To be added prior to presentation at the PAC